

PAIN

A ligand-receptor interactome platform for discovery of pain mechanisms and therapeutic targets

Andi Wangzhou, Candler Paige, Sanjay V. Neerukonda, Dhananjay K. Naik, Moeno Kume, Eric T. David, Gregory Dussor, Pradipta R. Ray*, Theodore J. Price*

Copyright © 2021
The Authors, some
rights reserved;
exclusive licensee
American Association
for the Advancement
of Science. No claim
to original U.S.
Government Works

In the peripheral nervous system, ligand-receptor interactions between cells and neurons shape sensory experience, including pain. We set out to identify the potential interactions between sensory neurons and peripheral cell types implicated in disease-associated pain. Using mouse and human RNA sequencing datasets and computational analysis, we created interactome maps between dorsal root ganglion (DRG) sensory neurons and an array of normal cell types, as well as colitis-associated glial cells, rheumatoid arthritis-associated synovial macrophages, and pancreatic tumor tissue. These maps revealed a common correlation between the abundance of heparin-binding EGF-like growth factor (HBEGF) in peripheral cells with that of its receptor EGFR (a member of the ErbB family of receptors) in DRG neurons. Subsequently, we confirmed that increased abundance of HBEGF enhanced nociception in mice, likely acting on DRG neurons through ErbB family receptors. Collectively, these interactomes highlight ligand-receptor interactions that may lead to treatments for disease-associated pain and, furthermore, reflect the complexity of cell-to-neuron signaling in chronic pain states.

INTRODUCTION

Nociceptive sensory neurons are responsible for detecting changes in the environment through specific receptors and then transmitting this signal to the central nervous system by generation of action potentials (1). These nociceptors innervate almost every tissue in the body, playing a critical role in detecting injury and/or pathology to skin, joints, bones, and visceral organs (2, 3). Although nociceptor function is needed to navigate environments safely (4) and to recover after injury (5), these cells can also create misery when they become persistently active (6–8). Nociceptor hyperexcitability and spontaneous activity are key contributors to many chronic pain states driven by inflammation, arthritis, nerve injury, cancer, or other pathologies (1, 2, 6–8). It is widely accepted that tissue injury is directly linked to changes in the activity of nociceptors that innervate that tissue (9). Relatively little is known about the factors that are released by cells within specific tissues and how these factors act on the nociceptors innervating the tissue. Our goal was to catalog this potential “interactome” because such a resource can suggest identification of previously unknown targets that could be manipulated to treat pain disorders.

RNA sequencing (RNA-seq) experiments have defined tissue-wide and cell-specific transcriptomes for much of the body in both mice (10–12) and humans (13, 14). Cell profiling experiments on normal and diseased tissues have identified key molecular players in an increasing number of disease processes (15), including disorders with a strong pain component (16, 17). However, these studies mostly focus on gene expression within a specific tissue or across cell types in a tissue and do not characterize how multiple tissues may interact to promote disease. This type of cross-tissue interaction is especially critical to pain. Nociceptors express a wide variety of receptors that allow them to detect ligands that are produced in the tissues that they innervate (1–3). Tissue pathology frequently drives changes in gene expression resulting in de novo or enhanced expression of ligands (for example, cytokines and chemokines). Because many pathological

tissue states produce enhanced nociception and pain (1, 5, 9), it is logical to assume that changes in ligand expression cause changes in signaling frequency or intensity through receptors expressed by nociceptors. These ligand-receptor interactions are candidates for drivers of pain states.

Here, we developed a computational framework that identified potential ligand-receptor-mediated interactions on a genome-wide scale (interactome) between target tissues and sensory neurons using publicly available RNA-seq datasets. We first used this tool to identify potential interactions between nociceptors in mouse dorsal root ganglia (DRGs) and other tissues or cell types. Then, we performed three case studies to demonstrate the utility of this tool for identifying potential drivers of pain states. First, we used single-cell RNA-seq (scRNA-seq) data from colon-innervating nociceptors in the mouse (17) to explore how these neurons might interact with normal and inflamed enteric glial cells (18). Second, we examined how human DRG (hDRG) neurons (14, 19) may interact with macrophages taken from the joints of people with rheumatoid arthritis (RA) (16). Last, we assessed how pancreatic cancer (20) could drive ligand-receptor interactions with hDRG neurons, potentially providing new insight into tumor-neuron interactions in this notoriously painful disease. An intriguing theme emerging from these distinct interactomes is the prominence of corresponding ligands for the ErbB family of epidermal growth factor receptors (EGFRs) as possible mediators of interactions between diseased tissue and mouse and human nociceptors. This finding is consistent with recent preclinical and clinical findings suggesting efficacy of blocking ErbB family signaling for chronic pain (21–24). As RNA-seq resources continue to proliferate, our tool can be used to mine for potential signaling pathways and pharmacological targets in a data-driven manner based on high-throughput assay analyses.

RESULTS

Cell type-enriched interactomes for DRG nociceptors from 42 cell types in the Tabula Muris dataset

DRG neurons interact with nearly every tissue in the body and express an array of receptors that enable them to receive signals from

School of Behavioral and Brain Sciences and Center for Advanced Pain Studies, University of Texas at Dallas, 800 W Campbell Rd., Richardson, TX 75080, USA.

*Corresponding author. Email: prr105020@utdallas.edu (P.R.R.); theodore.price@utdallas.edu (T.J.P.)

distinct cell types within these tissues (2, 3). To map these potential ligand-receptor interactions, we curated a database of ligand and receptor pairs across the genome, on the basis of the literature and curated bioinformatics databases (25–30). This led to the creation of a ligand-receptor pair interactome containing more than 3000 interactions.

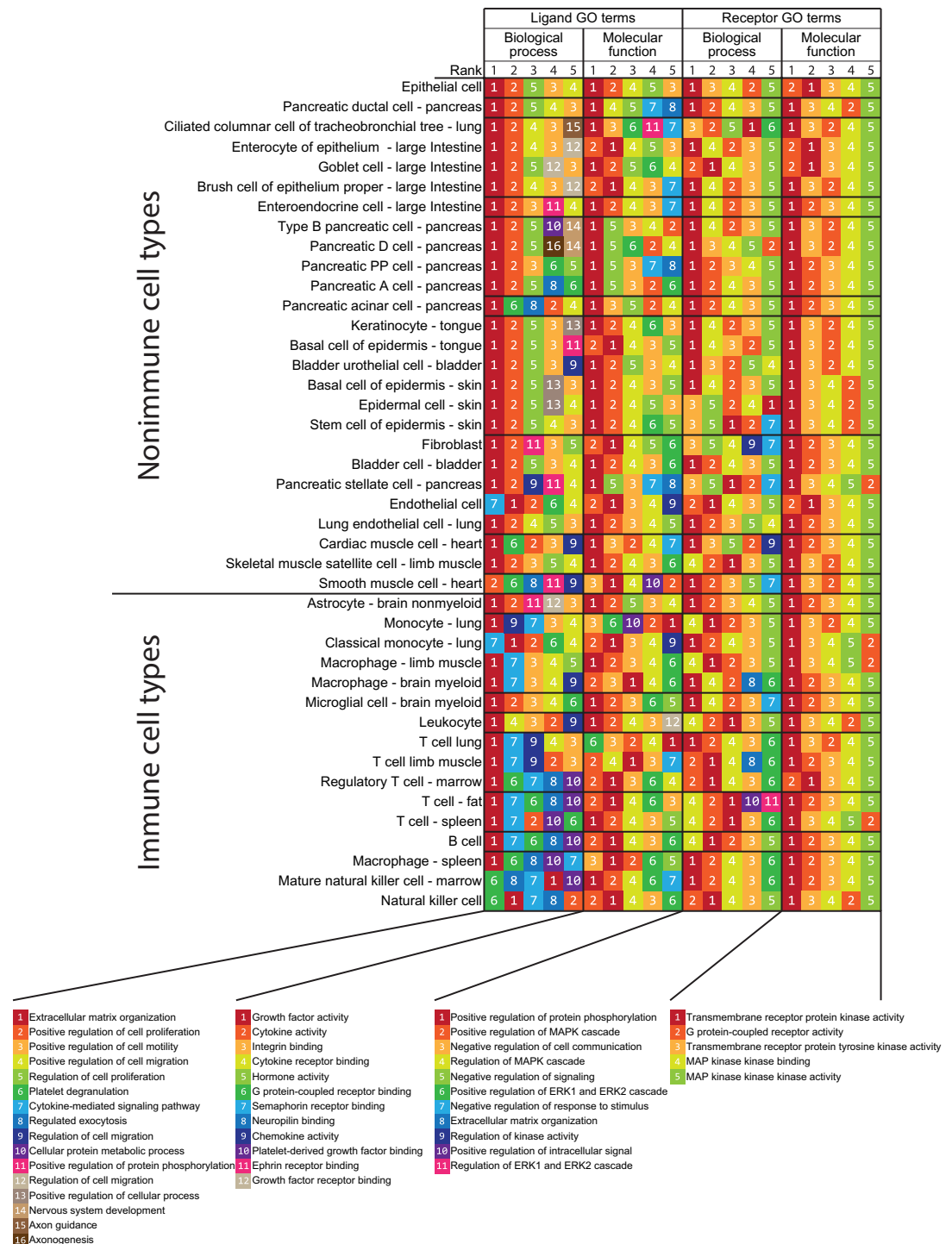
We first sought to examine ligand-receptor interactions between different classes of mouse sensory neurons and a diverse array of peripheral cell types under normal conditions. To do this, we used mouse DRG (mDRG) scRNA-seq data (12) and scRNA-seq datasets from tissues innervated by the DRG using the Tabula Muris project (10). Although many subtypes of sensory neurons have been identified (11, 12), for simplicity, we clustered these into three well-identified neuronal subpopulations: peptidergic (PEP) nociceptors; nonpeptidergic (NP) nociceptors; and neurofilament (NF)-positive, large-diameter, low-threshold mechanoreceptors (1–3). This predicted a broad interactome between 42 cell types found in 19 tissues, and PEP, NP, and NF sensory neurons from the DRG, and established a ligand-receptor interaction map for sensory neurons and the tissues they innervate or interact with in the mouse (data file S1). We extracted the pairs of ligand-receptor interactions for each of these cell types where the receptor was expressed in at least one type of sensory neuron (PEP, NP, or NF) and looked for enriched pharmacology-relevant Gene Ontology (GO) terms using the Enrichr analysis tool (31, 32), focusing on the top five GO terms for biological process (large-scale “biological programs” accomplished by several coordinated molecular activities) and molecular function (molecule-level activities performed by gene products, for instance) (Fig. 1). For the biological process GO terms found for ligand genes, the “extracellular matrix organization” term appeared in the top five for all but one cell type and was ranked as the top one in 37 of the 42 cell types. This likely occurred because among the 894 ligand genes that we included in the interactome, many are secreted and 89 of them are among the 229 total genes classified under the biological process GO term “extracellular matrix organization.” This biases our dataset to show this particular GO term to be enriched. The GO terms of “positive regulation of cell proliferation,” “regulation of cell proliferation,” “positive regulation of cell motility,” and “positive regulation of cell migration” were also enriched in both nonimmune cell types and macrophages. For terms that were enriched specifically in immune cells, “cytokine-mediated signaling pathway” was enriched in most of the immune cell types, whereas “regulated exocytosis” and “cellular protein metabolic process” GO terms were specific to T cells and natural killer (NK) cells (Fig. 1). This shows that, for most cell types, extracellular matrix (ECM) and cell adhesion ligands represent the most abundant ligand-receptor interaction between these peripheral cells and sensory neurons. The exception was immune cells, which our interactome predicts to primarily interact with sensory neurons through diffusible factors.

For receptor genes found in sensory neurons, the same five GO terms were enriched for molecular functions: “transmembrane receptor protein kinase activity,” “G protein-coupled receptor activity,” “transmembrane receptor protein tyrosine kinase activity,” “mitogen-activated protein (MAP) kinase kinase binding,” and “MAP kinase kinase activity” (Fig. 1). The biological process GO terms were also consistent for sensory neuron receptors identified from this interactome. The same four GO terms were enriched for most of the cell types: “positive regulation of protein phosphorylation,” “positive regulation of MAPK cascade,” “negative regulation of cell

communication”, and “regulation of MAPK cascade.” Two other GO terms, “negative regulation of signaling” and “positive regulation of ERK1 and ERK2 cascade,” were enriched in nonimmune cell types and macrophages or T cells and NK cells, respectively. This highlights the key role that MAPK (mitogen-activated protein kinase) signaling plays in transducing signals from cells throughout the body to signaling within sensory neurons. Because MAPK signaling in nociceptors plays a critical role in the generation of pain states (33–36), this suggests that ligand-receptor interactions between nociceptors and most cell types found in the body could be capable of inducing hyperexcitability in nociceptors leading to persistent pain.

Although the interactome described above shows commonalities between ligand-receptor interactions between sensory neurons and a variety of tissues and cells found in the mouse, it does not reveal cell type-specific interaction points that may play important roles in normal physiology and/or pathology. To find these more specific interactions in an unbiased fashion, we performed iterative hierarchical biclustering on cell types and genes based on gene expression levels using *scratch.hicat* analysis (37). This analysis revealed 18 classes of cell types (cell clusters A to R in Fig. 2A) and 25 gene coexpression modules expressed across subsets of those cell types (Fig. 2A). For each of these 25 gene modules, we then extracted all the ligand genes from our ligand-receptor database for each module and constructed an interactome with receptors expressed by different classes of mouse sensory neurons (data file S2). We focused on two module interactomes enriched in immune cell types for graphical representation: the macrophage- and leukocyte-enriched cluster, and the T cell- and NK cell-enriched cluster. We chose these on the basis of the key role that these immune cell types play in neuropathic pain models in male and/or female mice (38–43). The ligand-receptor interactomes emerging from this gene cluster enrichment analysis revealed distinct factors expressed by these immune cells that are known to play a role in neuropathic pain states. The macrophage and leukocyte cluster included *Mmp9*, *Il1b*, and *Osm* gene products signaling to their cognate receptors expressed by mouse nociceptors (Fig. 2B). Macrophage recruitment by tumor necrosis factor- α (TNF- α) induces matrix metalloproteinase MMP9 signaling, which then promotes neuropathic pain after peripheral nerve injury (44). Cytokines interleukin-1 β (IL-1 β) and oncostatin M (OSM) have also been identified as important pain signaling molecules in previous studies in rodent pain models (45, 46) and in DRG samples from patients with neuropathic pain (19). The T cell and NK cell cluster not only showed expression of many genes associated with the TNF- α superfamily, including *Lta*, *Tnfsf14*, and *Tnfsf11*, but also highlights the *Ltbr* gene, which is paired with several of these T cell- and NK cell-expressed ligands (Fig. 2C). This analysis also identified a specific interaction between T cells and sensory neurons driven by the action of interferon- γ (IFN- γ) through its receptors (IFNGR1 and IFNGR2) expressed on sensory neurons. IFN- γ had previously been shown to enhance glutamate release in excitatory synapses in spinal cord and contributes to persistent pain (47). Collectively, this previous work implicates these factors in persistent pain, but our analysis shows that these immune cells express these factors at baseline. This suggests that recruitment of these immune cells to the peripheral nerve may be a key factor in driving persistent pain rather than plasticity in the transcriptomes of these cell types. This notion is supported by recent studies in rodent models (40, 41, 43) and patient transcriptional profiling (19). This cell type and gene module biclustering approach reveals potential ligand-receptor interactions

Fig. 1. GO and interactome analysis of ligand and receptor gene expression reveals shared principles of cell-to-neuron signaling across tissues. Interactome analysis was performed between all 42 peripheral cell types from the Tabula Muris project (10) and three types of sensory neurons (11, 12). Only interactions where ligands were detected in the corresponding cell type and receptors were detected in at least one of the three sensory neuron types were included for the GO term enrichment analysis. For the interactions identified in each cell type, the corresponding ligand and receptor genes were separately analyzed with Enrichr for their enriched GO terms in both biological process and molecular function. The results of this analysis are shown in four different groups of columns. The five columns of color- and number-coded boxes within each of these four groups of columns represent the top five enriched GO terms in that group, ranked from left to right. Cell types are listed as rows and ordered by the cell type and gene biclustering, as described in Materials and Methods. *N* = 889 cells for NP-type DRG, 126 cells for NF-type DRG, and 565 cells for PEP-type DRG neurons; sample sizes for other cell types are provided in data file S7.



Downloaded from <http://stke.sciencemag.org> on July 28, 2021

for peripheral cell types with sensory neurons that can be further mined for identification of new pain targets.

Ligand-receptor interactions among cell types within the mDRG are identified from the mousebrain.org dataset

The interactomes described above map ligand-receptor pairs between sensory neurons and many other cell types found in target tissues for these neurons. The DRG is composed of many different cell types

besides sensory neurons, including Schwann cells and satellite glial cells. These glial cells are known to contribute to acute and chronic pain states (48–50), but how they interact with sensory neurons has not been characterized thoroughly. Moreover, how sensory neurons may interact with these cells through release of transmitter substances is almost completely unexplored. To examine ligand-receptor interactions that might occur within the DRG, we constructed ligand-receptor interactomes between NP, PEP, and NF sensory neurons

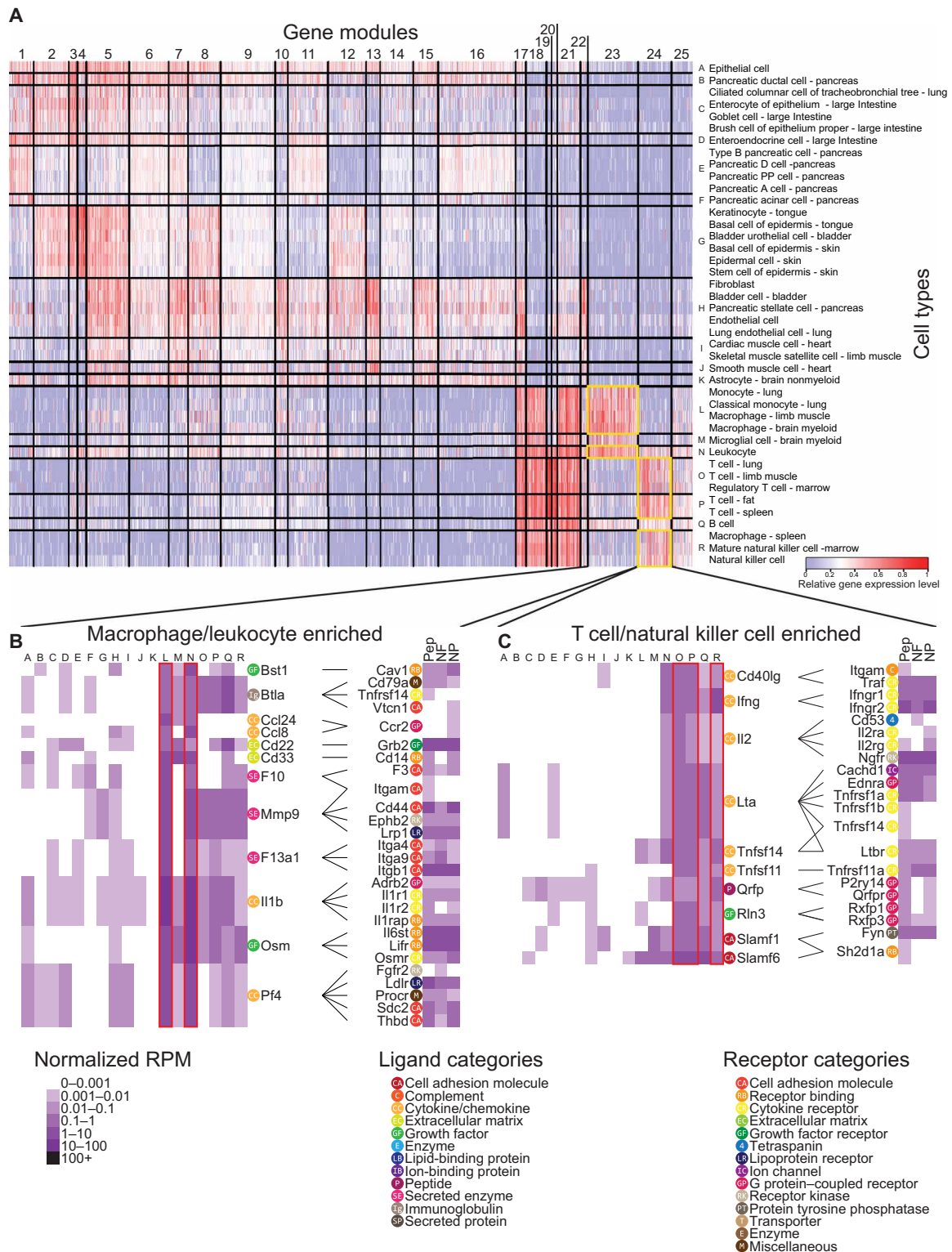


Fig. 2. Potential cell type-specific ligand-receptor interactions with sensory neurons. (A to C) Iterative hierarchical biclustering was performed on genes and cell types from mouse scRNA-seq gene expression data in Tabula Muris (10) using scratch.hicat (37). The 42 cell types grouped into 18 cell-type modules and 25 gene modules [labeled “A” to “R” and “1” to “25,” respectively, in (A), and listed in data file S2] were identified, and corresponding gene expression was displayed as a heatmap. Two of these gene modules, numbers 23 and 24—ligand genes enriched in macrophages and leukocytes [cell-type modules L and N; (B)] or in T cells and NK cells [cell-type modules O, P, and R; (C)], as outlined—are highlighted below, alongside DRG receptor expression heatmaps (12) and annotated with potential ligand-receptor interactomes. Gene categories as labeled are defined in the figure legend. For DRG neurons: *N* = 889 cells for NP, 126 cells for NF and 565 cells for PEP; sample sizes for other cell types provided in data file S7.

and satellite glial cells and Schwann cells. We did this with scRNA-seq data from the mousebrain.org dataset (12). In our first analysis of this interactome, it was clear that “cell adhesion molecule and extracellular matrix” categories dominated the ligand-receptor interactions for these cell types (data file S3 and figs. S1 and S2). This is not unexpected, given the close proximity of these cells within the DRG and the obvious structural role that interactions between these cells play within the ganglion. The role of cell adhesion molecules and ECM molecules in chronic and neuropathic pain has been described in the literature (51, 52). However, because we wanted to focus on interactions driven by diffusible transmitter substances within the DRG, we chose to remove these two categories from this analysis of intercellular ligand-receptor signaling within the mDRG. These categories are included in subsequent analyses.

When examining which neuronal ligands potentially signal to satellite glia and/or Schwann cell-expressed receptors, we made several interesting observations (Fig. 3). First, growth factor interactions were the dominant category of interactions when considering neuron to glial signaling, with 30 of the 133 interactions being between growth factors and their receptors. This is consistent with previous findings in the field (53–55). Second, we found indications of robust brain-derived neurotrophic factor (BDNF) signaling within the DRG. We noted that gene products of *Bdnf*, which was expressed by NP and PEP nociceptors, has potential interactions with satellite glia and Schwann cells through its traditional receptor tropomyosin/tyrosine receptor kinase B (TrkB, encoded by *Ntrk2*), as well as through discoidin domain-containing receptor 2 (DDR2, encoded by *Ntrkr3r*) and sortilin (encoded by *Sort1*). Last, we found that calcitonin gene-related peptide (CGRP, encoded by *Calca*), a signature peptide of PEP nociceptors, had an interaction with the amylin receptor activity modifying protein 2 (RAMP2) in DRG glia cells. Although it is known that CGRP can signal through receptors containing the amylin subunit (56), there is no previous literature on CGRP signaling through this receptor in DRG glia.

We then assessed DRG glial ligand signaling to neuronal receptors. This interactome was more diverse and revealed an increased number of these interactions. There were 133 neuronal ligands interactions with glial receptors; conversely, there were 199 glial ligand and neuronal receptor interactions. Whereas the classes of ligands coming from glia did not fall into one main category, 56 of the 199 receptors for neurons were composed of G protein-coupled receptors (GPCRs), ion channels, or cytokine receptors (Fig. 4). A prominent ligand-receptor interaction emerging from this dataset was the broad expression of platelet-derived growth factor (PDGF) family genes in satellite glial cells and Schwann cells, gene products of which signal to a single neuronal receptor whose gene (*Pdgfrb*) expression is enriched in the NP class of nociceptors. Although PDGF is known to sensitize nociceptors leading to increased mechanical sensitivity (57, 58), little work has been done on PDGF signaling within the DRG, making this an attractive target for further exploration. When comparing these two sets of data, it is notable that there was an enormous variety in the interactions between glial ligands and neuronal receptors. Our data support previous findings in the literature regarding neuronal signaling in the DRG while identifying potential new interactions that will need further investigation. In the mDRG, we find similar neuron–glia ligand–receptor interaction profiles for PEP and NP nociceptors but several differences between non-nociceptive NF neurons and nociceptors (Fig. 4). An example is Schwann cell- and satellite glial cell-derived PDGF signaling to one of its receptors, PDGFRB, which was exclusively found in NP neurons.

An interactome between enteric glia and colon-innervating nociceptors defines gut-neuron interactions in a colitis model

Thus far, we have described interactomes between peripheral tissues and DRG neurons, as well as within the DRG, by using sequencing experiments from naïve mice. Certain ligand-receptor interactions may not exist in this state and may only be revealed during pathology where those interactions play a critical role in promoting disease. This principle is the basis of the use of most drugs that are used to treat disease. To explore how the ligand-receptor interactome of DRG sensory neurons changes in a disease state, we examined how colonic enteric glial cells react and communicate with retrogradely labeled and single-cell sequenced sensory neurons innervating the colon (17) in the mouse 2,4-di-nitrobenzene sulfonic acid (DNBS) colitis model. We used an existing dataset of RiboTag RNA-seq of enteric glial cells in this colitis model (18), because this technique affords cellular specificity combined with an in vivo inflammatory disease model. An scRNA-seq dataset of retrogradely traced sensory neurons that innervate the colon was chosen because these cells make contact with enteric glia and are at least partially transcriptomically distinct from other DRG sensory neurons (17).

Transcriptomic changes in the DNBS-treated enteric glial dataset were evaluated first. Differential gene expression analysis was performed between vehicle and DNBS-treated groups to identify genes with substantial differences in abundance. This gene list was then intersected with our interactome analysis against retrogradely traced, mouse colonic sensory neuron scRNA-seq data. The original study identified seven cell types from these retrogradely traced mouse colonic sensory neurons. These cell types were defined by expression profiles (NP, PEP, and NF), and they were further defined by their anatomical location (either thoracolumbar and lumbosacral DRG, or lumbosacral only) (17). We separated these into five cell types that were found in both thoracolumbar and lumbosacral DRGs (hereafter and in the figure denoted as mixed populations; Fig. 5A) and two cell types that were only found in lumbosacral DRG (pelvic populations; Fig. 5A). The interactome between differentially expressed ligands in DNBS-treated enteric glia and paired receptors enriched in one of these seven cell types are presented (Fig. 5A and data file S4, sheet 1), with ligand-receptor pairs that did not show any DRG neuron enrichment for any of the seven cell types are shown in the Supplementary Materials (data file S4, sheet 2). We found that for 17 of 22 interactions where the receptor gene was enriched in the two pelvic specific cell types, their ligand-pair gene expression was substantially decreased. In contrast, in 39 of 64 interactions where the receptor gene was enriched in mixed DRG cell types, their paired ligand gene expression was substantially increased. Under the premise that increased gene (and potentially protein) abundance leads to increased protein interactions, this shows that there is a potential difference in signaling between enteric glia and colonic sensory neurons wherein inflammation relatively specifically augments ligand-receptor interactions between mixed population afferents, whereas there is a tendency of decrease in interactions between enteric glia and pelvic afferents (Fig. 5B).

On the basis of the premise that elevated gene abundances could cause robust protein interactions and may be important for pelvic pain disorders, we looked more closely at this part of the interactome. Among increased ligand genes that signaled to DRG neurons in the mixed population, we found that *Bdnf* and *Gdnf* were prominent. BDNF signaling to TrkB is known to play an important role in pain

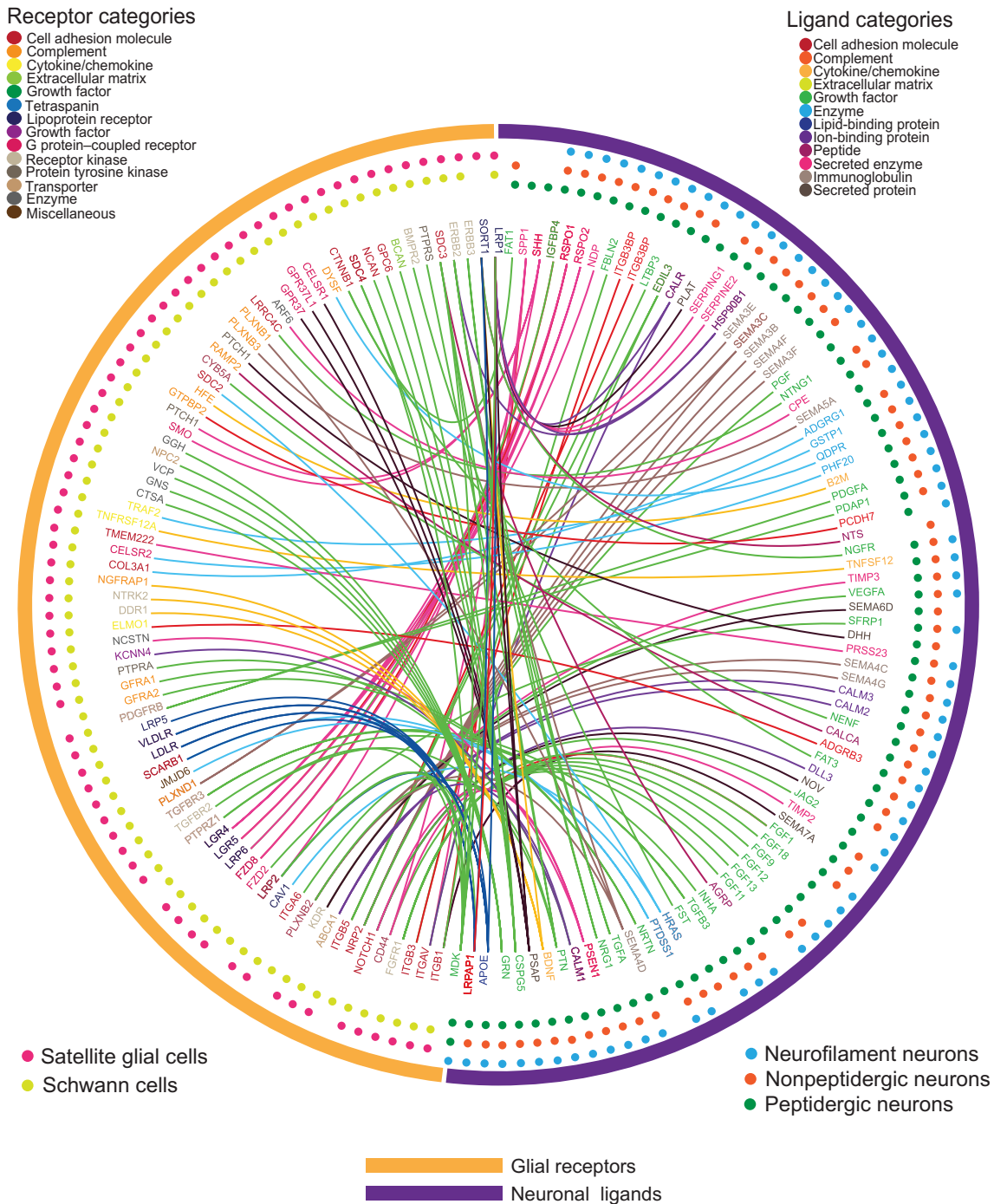


Fig. 3. Ligand-receptor interactions from neurons to glial cells within the DRG. Interactome analysis was performed to identify potential signaling connections between ligands expressed by DRG neurons [PEP-type ($n = 565$ cells), NP-type ($n = 889$ cells), and NF-type ($n = 126$ cells)] and the paired receptor expressed by DRG glial cells [satellite glia ($n = 681$ cells) and Schwann cells ($n = 47$ cells)] from the mouse scRNA-seq dataset by Zeisel *et al.* (12). Outermost circles indicate the generic class of the cells expressing the corresponding ligand or receptor genes. The middle layer shows the specific cell type that the gene is detected in, with the dots color-coded for cell type. The inner layer contains gene names, color-coded for their corresponding ligand or receptor categories. Connections are marked as lines between ligand genes and receptor genes, color-coded for the neuron-expressed ligand gene category.

plasticity where it has primarily been studied in the context of BDNF release from primary afferents in the spinal cord (59, 60) but has also been linked to inflammatory visceral pain disorders (61–63). Glial cell line-derived neurotrophic factor (GDNF), which was linked

to *Gfra1* and *Gfra2* expression, was also found to be increased in relative gene abundance in DNBS-treated enteric glial cells. Other studies have indicated that GDNF up-regulation in target tissues enhances nociception (64–66). ARTN (artemin), a ligand in the same

Ligand categories

- Cell adhesion molecule
- Complement
- Cytokine/chemokine
- Extracellular matrix
- Growth factor
- Enzyme
- Lipid-binding protein
- Ion-binding protein
- Peptide
- Secreted enzyme
- Immunoglobulin
- Secreted protein

Receptor categories

- Cell adhesion molecule
- Receptor binding
- Cytokine receptor
- Extracellular matrix
- Growth factor receptor
- Tetraspanin
- Lipoprotein receptor
- Ion channels
- G protein-coupled receptor
- Receptor kinase
- Protein tyrosine phosphatase
- Transporter
- Enzymes
- Miscellaneous

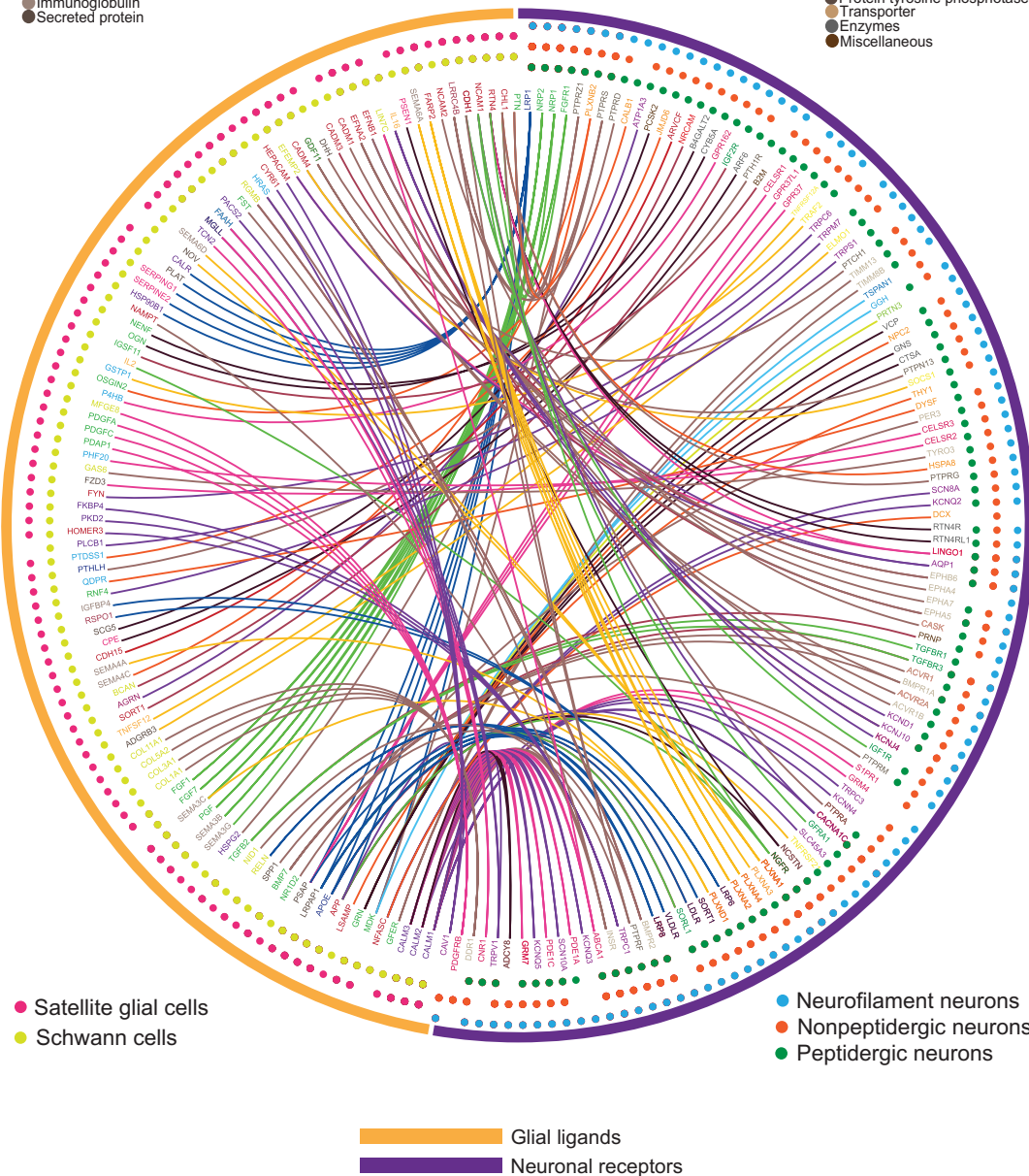


Fig. 4. Ligand-receptor interactions from glial cells to neurons within the DRG. Interactome analysis was performed to identify potential signaling connections between ligands expressed by glial cells [satellite glia ($n=681$ cells) and Schwann cells ($n=47$ cells)] and the paired receptor expressed by DRG neurons [PEP-type ($n=565$ cells), NP-type ($n=889$ cells), and NF-type ($n=126$ cells)] from the mouse scRNA-seq dataset by Zeisel *et al.* (12). Outermost circles indicate the generic class of the cells expressing corresponding ligand or receptor genes. The middle layer shows the specific cell type that the gene is detected in, with the dots color-coded for cell type. The inner layer contains gene names, color-coded for the corresponding ligand or receptor categories. Connections are marked as lines between ligand genes and receptor genes, color-coded for the neuron-expressed receptor gene category.

pain. However, discoveries made in mouse models are not always consistent with actual human disease states (68, 69). Therefore, we sought to assess whether this interactome approach could be used to identify novel targets in human disease states. This requires availability of hDRG sequencing data and sequencing data from target tissues or cells from patients with chronic pain diseases. We chose to investigate how macrophages from RA patient synovium might communicate with cell types in the hDRG, especially human sensory neurons.

family as GDNF, was also found to be increased in gene expression and linked with *Gfra1* and *Gfra3* expression. This demonstrates a coordinated increased expression of neurotrophins in enteric glia that are likely to signal through pelvic and lumbosacral mechanisms to promote visceral pain (61–67).

Disease-promoting macrophages from patients with RA interact with hDRG through an EGFR-enriched pathway

The interactome analysis described above shows that we can identify ligand-receptor signaling pathways in a mouse model of visceral

A previously published scRNA-seq study of synovial tissue from patients with RA and osteoarthritis (OA) identified four specific subtypes of macrophages within the joints of patients with either of these diseases (16). A total of 12 patients with RA (7 females and 5 males) and 2 patients with OA (both male) were enrolled in the study by Kuo *et al.* (16). To find macrophage-driven interactions with hDRG neurons that are potentially responsible for promoting pain in RA, we contrasted the RA-enriched macrophage cell types with the OA-enriched macrophage cell types. Ligand genes that were highly expressed in the RA macrophages compared with the

Downloaded from <http://stke.sciencemag.org> on July 28, 2021

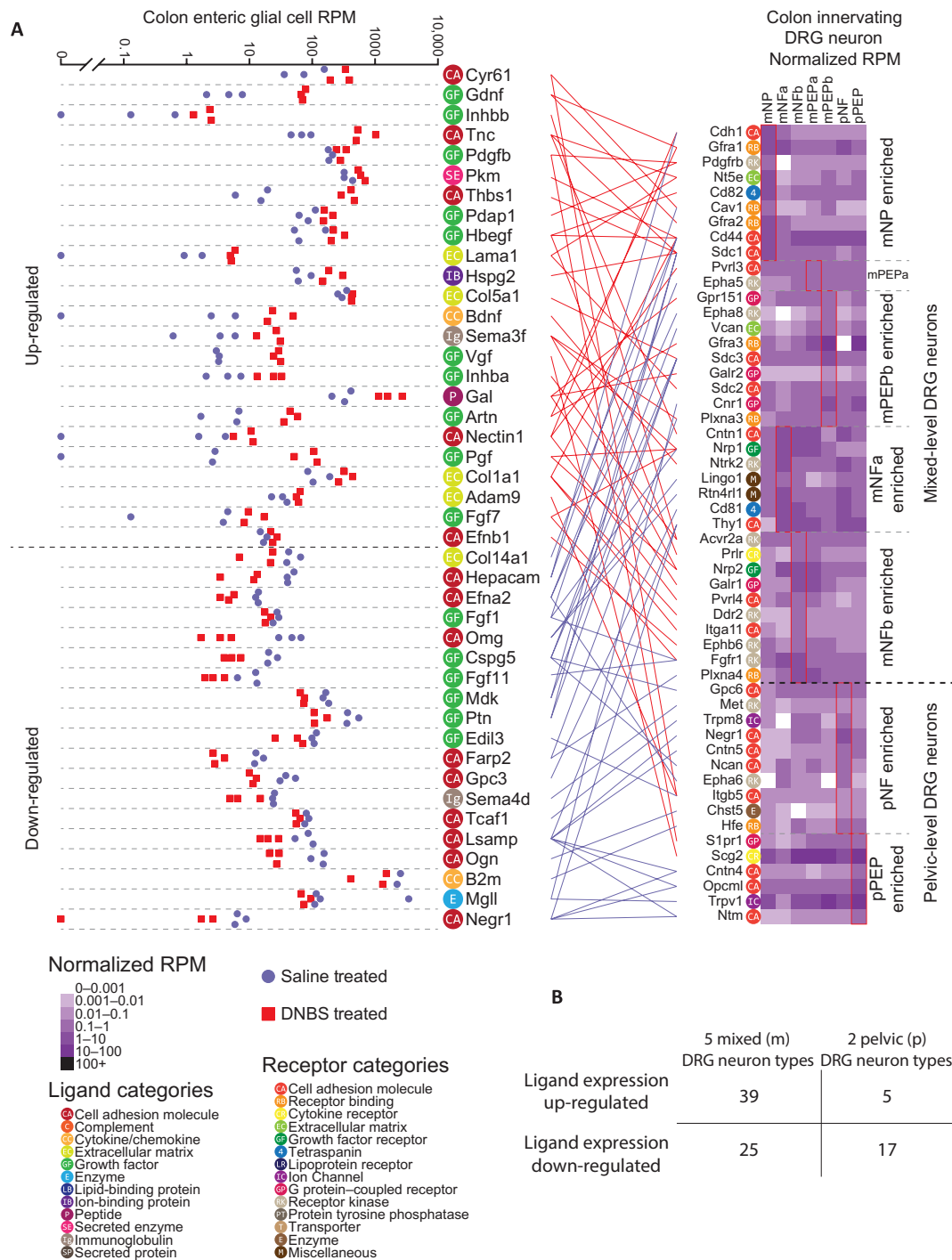


Fig. 5. Differential expression and interactome analysis of ligands in enteric glia and of receptors in colon-projecting sensory neurons reveal potential drivers of visceral pain. (A) Differential expression of ligand-encoding genes in RiboTag RNA-seq of enteric glial cells from mice treated with saline or DNBS ($N=3$ each) (18) and gene expression of corresponding receptor-encoding genes in scRNA-seq of DRG sensory neurons (314 cells) (17), grouped by type as indicated. Ligand-receptor pairs between the enteric glia and colon-innervating neurons are connected between the plots, wherein red (above the dashed line in the plot, left) indicates ligand expression was increased in enteric glial cells after DNBS treatment, and blue indicates a decrease. Ligand and receptor genes are labeled with color-coded category labels, defined in the figure legend. Cell types prefixed with “p” denote populations primarily from lumbosacral (pelvic) DRG, whereas those prefixed with “m” denote populations sampled from a mixture of thoracolumbar and lumbosacral DRG. (B) Table enumerating the number of glia-expressed ligands—those that were up-regulated and, separately, down-regulated in DNBS-treated animals—that corresponded to receptors in the indicated grouped subtypes of DRG neurons.

OA macrophages were selected and then filtered by whether their receptor genes were detected in hDRG RNA-seq data (14, 19), resulting in RA-enriched ligand-receptor pairs (Fig. 6). OA-enriched interactions—which include pathways related to bone regeneration—are in the Supplementary Materials (data file S5). Of the 20 RA-enriched ligand-encoding genes, four of them—*HBEGF*, *EREG*, *DCN*, and *HSP90AA1*—encode proteins that signal through EGFR. This suggests that ErbB family receptors may play a key role in promoting persistent pain in patients with RA. Increased expression of ErbB

family-related ligands and receptors is seen in patients with RA. For instance, ErbB family pathway changes are triggered by increased abundance of amphiregulin and epiregulin (EREG) in patients with RA (70), whereas experiments in mice have shown the development of cytokine-induced arthritis can be suppressed with local blockade of these ligands in the joint (71). The importance of the ErbB family pathway in chronic pain has been previously noted in the literature, but not in the context of RA pain. For instance, EREG-mediated EGFR activation causes pain sensitization through

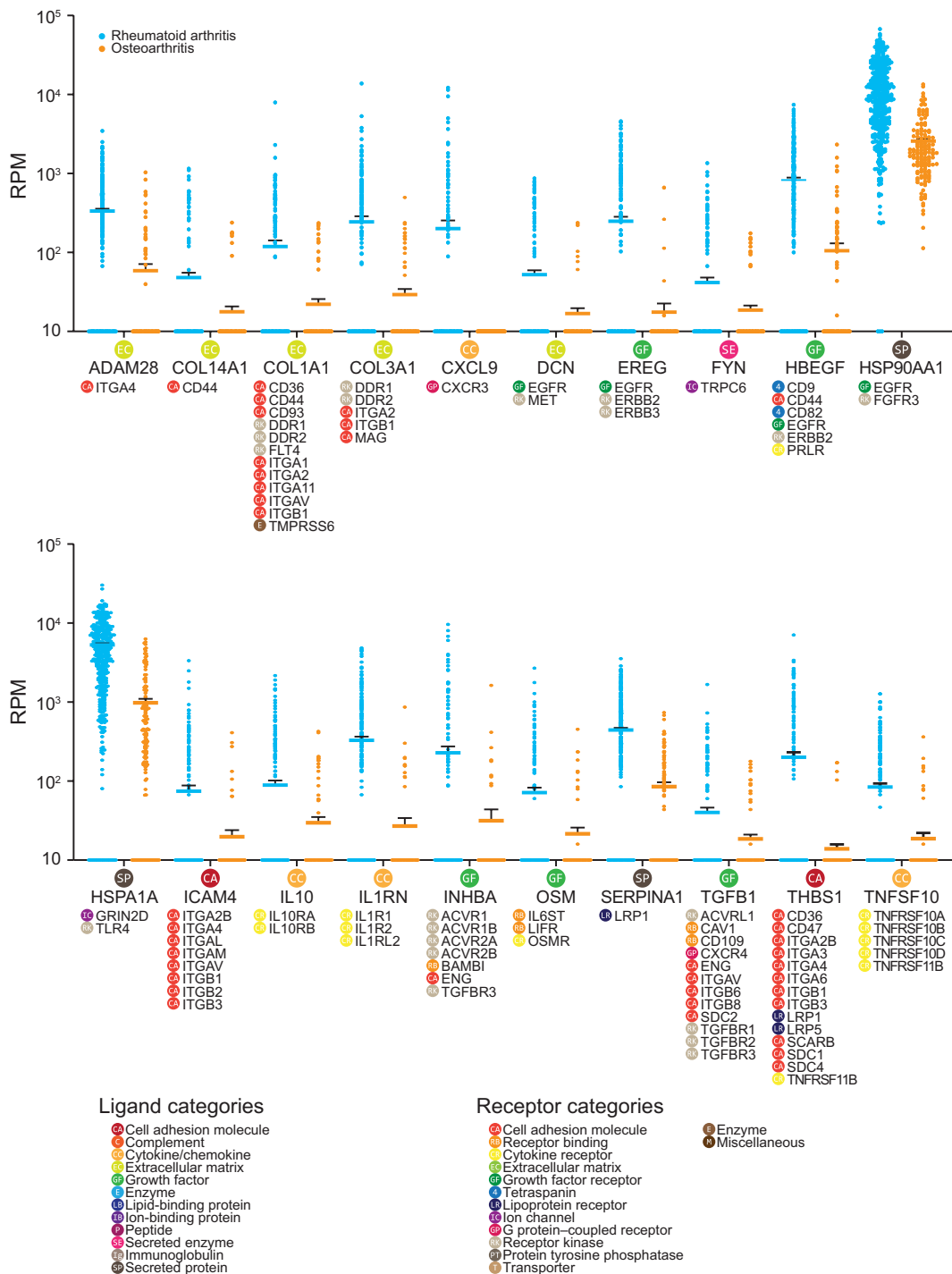


Fig. 6. DRG receptor-associated ligand expression in synovial joint macrophages identifies potential drivers of persistent pain in RA. Differential expression of ligand-encoding genes in synovial macrophages isolated from patients with RA (394 cells) and those isolated from patients with OA (139 cells), based on human scRNA-seq data from Kuo *et al.* (16). Only ligand genes with higher expression level in RA macrophages compared with OA macrophages are shown. Gene expression level in RPMs for each cell is shown (RA macrophages in blue; OA macrophages in orange) with the solid line as the mean and error bars representing SEM. Corresponding receptor genes detected in hDRG (*N* = 3 from individual organ donors) are noted under each ligand gene. Corresponding ligand or receptor categories are color-coded and labeled for each ligand or receptor gene as shown in the legend.

phosphatidylinositol 3-kinase–AKT–mechanistic target of rapamycin pathways in inflammatory pain models (23) and EGFR inhibition with gefitinib reduces opioid tolerance and hyperalgesia

(72). Moreover, ErbB receptor family inhibitors have been used successfully for the treatment of neuropathic pain in patients (22, 24). RA treatment has been transformed by the use of TNF- α -targeting

biologics, but chronic pain remains a persistent problem for patients with RA (73, 74). With previous findings showing ErbB family inhibitors can be used to treat RA in mouse models (71, 75), we propose that inhibitors of the ErbB receptor family could potentially be repurposed to treat inflammation and RA pain at the same time.

Pancreatic cancer cells suppress inhibitory and enhance excitatory signaling to hDRG neurons

Pancreatic cancer involves cancer-driven mutational changes and large-scale transcriptional reprogramming. It is often associated with severe pain, and many patients are resistant to pharmacological pain treatment of any kind, requiring neurolytic treatments (76, 77). A better understanding of how cells from pancreatic cancerous tissue signal to DRG neurons could lead to identification of therapies that can alleviate pancreatic cancer pain.

We used a bulk RNA-seq dataset of pancreatic cancer tissue where we could control for individual differences in transcriptomes by having matched cancer and noncancer pancreatic samples from each of four patients (two females and two males) in the The Cancer Genome Atlas (TCGA) database (20). These four patients had stage II tumors (one of them in stage IIa and the other three in stage IIb). According to the definition of pancreatic cancer stages by the American Cancer Society, stage IIb pancreatic cancer has spread to no more than three nearby lymph nodes and may be considered as unresectable by physicians (www.cancer.org/cancer/pancreatic-cancer/detection-diagnosis-staging/staging.html). Over 80% of these patients with unresectable pancreatic cancer experience pain (78, 79). Ligands that systematically increased or decreased in abundance in cancer samples across all four patients were used for the interactome analysis. These interactions were then filtered by whether their receptor genes were detected in hDRG RNA-seq data (19). Among 41 ligand-receptor pairs identified (Figs. 7 and 8 and further detailed in data file S6), we noted that genes of certain mediators that are well-known pain suppressing ligands showed decreased expression in cancerous tissue compared with healthy tissue. These included the endogenous opioid ligand proopiomelanocortin and the anti-inflammatory cytokine IL-10. On the other hand, the expression of many pain-promoting and/or inflammatory ligand-encoding genes was increased, including *SHH*, *TGFA*, and *TFF1*. These findings suggest that a central problem in pancreatic cancer pain may be a loss of balance between pain-suppressing and pain-promoting signal transduction that is found within the normal pancreas. Four of these 41 ligand-encoding genes—*CEACAM1*, *FGF1*, *TFF1*, and *TGFA*—encode proteins known to signal through EGFR, suggesting (as above in RA) that the ErbB receptor family may play a role in driving pain in the context of pancreatic cancer. Although the corresponding ligands of ErbB receptor family members have been previously studied in the context of cancer (where EGFR and ErbB2 are known targets), they have not been widely studied in the context of pain. In addition, ErbB receptor family inhibitors have been shown to provide pain relief in previous cancer clinical trials (80). This may occur because of inhibition of tumor-to-nociceptor signaling or as tumor shrinkage decreases pressure on nearby nerves, like the celiac plexus.

HBEGF stimulates mDRG neurons and causes pain in vivo

Our results suggest a potential role of ErbB receptor family in many types of pain, but the only corresponding ligand that has been

confirmed to cause pain in vivo is EREG (23). To the best of our knowledge, heparin-binding epidermal growth factor (HBEGF) has never been assessed for pronociceptive actions, but our datasets suggest a possible role in several pain states. We applied HBEGF (10 ng/ml) to mDRG neurons from male and female mice and observed a Ca^{2+} signal in ~30% of neurons (Fig. 9, A and B). This effect was completely blocked by the ErbB family antagonist lapatinib (6 nM) (Fig. 9, C and D). Lapatinib blocks receptor kinase activity for both EGFR and ERBB2 (81). To examine the effect of HBEGF in peripheral tissues innervated by sensory nerve endings, we injected HBEGF (50 ng) into the paw of mice to test for mechanical sensitivity and grimacing. Male Institute of Cancer Research (ICR) and female C57BL/6 mice were used to test sex and strain differences. In male mice, we observed mechanical hypersensitivity (Fig. 9E) and a trend toward increased grimacing (Fig. 9F). In female mice, HBEGF also caused mechanical hypersensitivity (Fig. 9G) and grimacing at 1 hour after injection (Fig. 9H). Examining pooled data from male and female mice revealed a strong effect on mechanical hypersensitivity lasting for at least 24 hours (Fig. 9I) and a significant effect on grimacing at 1 hour after injection (Fig. 9J). Because responses were qualitatively similar between the two groups of mice, it is unlikely that there are major sex or strain differences in HBEGF responses in mice. We conclude that like EREG, HBEGF is an ErbB receptor family agonist that causes pain in vivo, likely through a direct action on ErbB2 receptors expressed by DRG nociceptors.

DISCUSSION

We have created an interactome identification framework for the examination of how specific subtypes of cells in the body interact with sensory neurons that innervate the target tissues where these cells reside. This resource can be used to mine interactions between sensory neurons and many of the cell types found in the bodies of mice. Many of these ligand-receptor interactions are generic; however, an unexpectedly large number of them show specificity. For instance, T cells and NK cells appear to use lymphotoxin alpha (*Lta*) to lymphotoxin beta receptor (*Ltbr*) as a unique mechanism to signal to nociceptors. Our work also elucidates how ligand-receptor interactions can potentially change in chronic pain disease states such as RA and pancreatic cancer. Our database and computational framework can be useful for identifying new targets for disease treatment (for example, HBEGF acting on ErbB receptors). We anticipate that continuing advances in sequencing techniques (82), such as spatial transcriptomics (83), and their application to human disease tissues will enable targeted therapeutic discoveries using this interactome framework.

One of the key findings emerging from our work is the complexity of the potential ligand-receptor interactions that are found in these interactomes. Pain is widely acknowledged to be a complex disease, but most pain therapeutic development focuses on a single factor, such as nerve growth factor (NGF) or CGRP sequestering antibodies, or receptor or enzyme antagonists (84). Some of these approaches, for instance, NGF (85) and CGRP (86) targeting, have been effective in the clinic. However, not all patients respond to these therapeutics and even when patients do respond, these therapies are not cures. Our work shows that chronic pain disease states are accompanied by complex changes in ligands produced in diseased tissues and that many of these ligands have considerable potential to have an action on the nociceptors that innervate that tissue. This likely means that

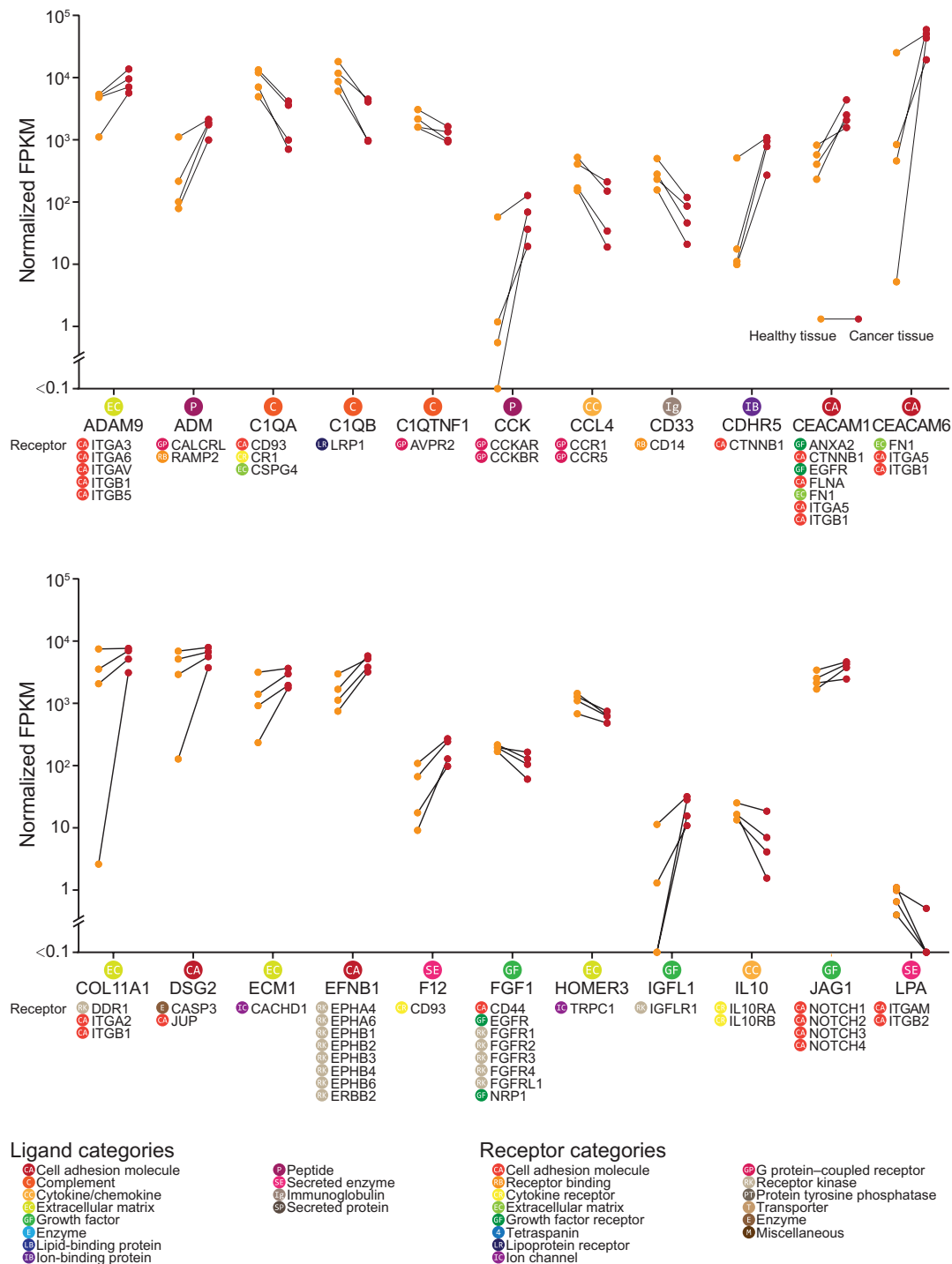


Fig. 7. DRG receptor-associated ligand expression in normal and malignant pancreatic tissue from humans, part I, reveals potential mediators of pancreatic cancer pain. Differential expression of ligand-encoding genes between healthy and cancerous tissue from four individuals with pancreatic carcinoma, obtained from the TCGA bulk RNA-seq datasets (20) and presented, in part, in alphabetical order. Only ligand genes with a corresponding receptor gene expressed in the hDRG dataset ($N = 3$ from individual organ donors) are shown. Gene expression level in FPKMs is shown (healthy tissue in orange; cancerous tissue in red) with the connected line marking the samples from the same patient. Corresponding receptor genes detected in hDRG are shown under each ligand gene. Corresponding ligand or receptor categories are color-coded and labeled for each ligand or receptor gene as shown in the legend.

multiple ligand-receptor interactions need to be simultaneously targeted to effectively treat chronic pain states. Of course, this is not a new concept, but our work starts to provide a toolkit to quantify

these ligand-receptor interactions and design therapeutic strategies that have an increased chance of success. Continuing to develop transcriptomic maps of human tissues, at the bulk and single-cell

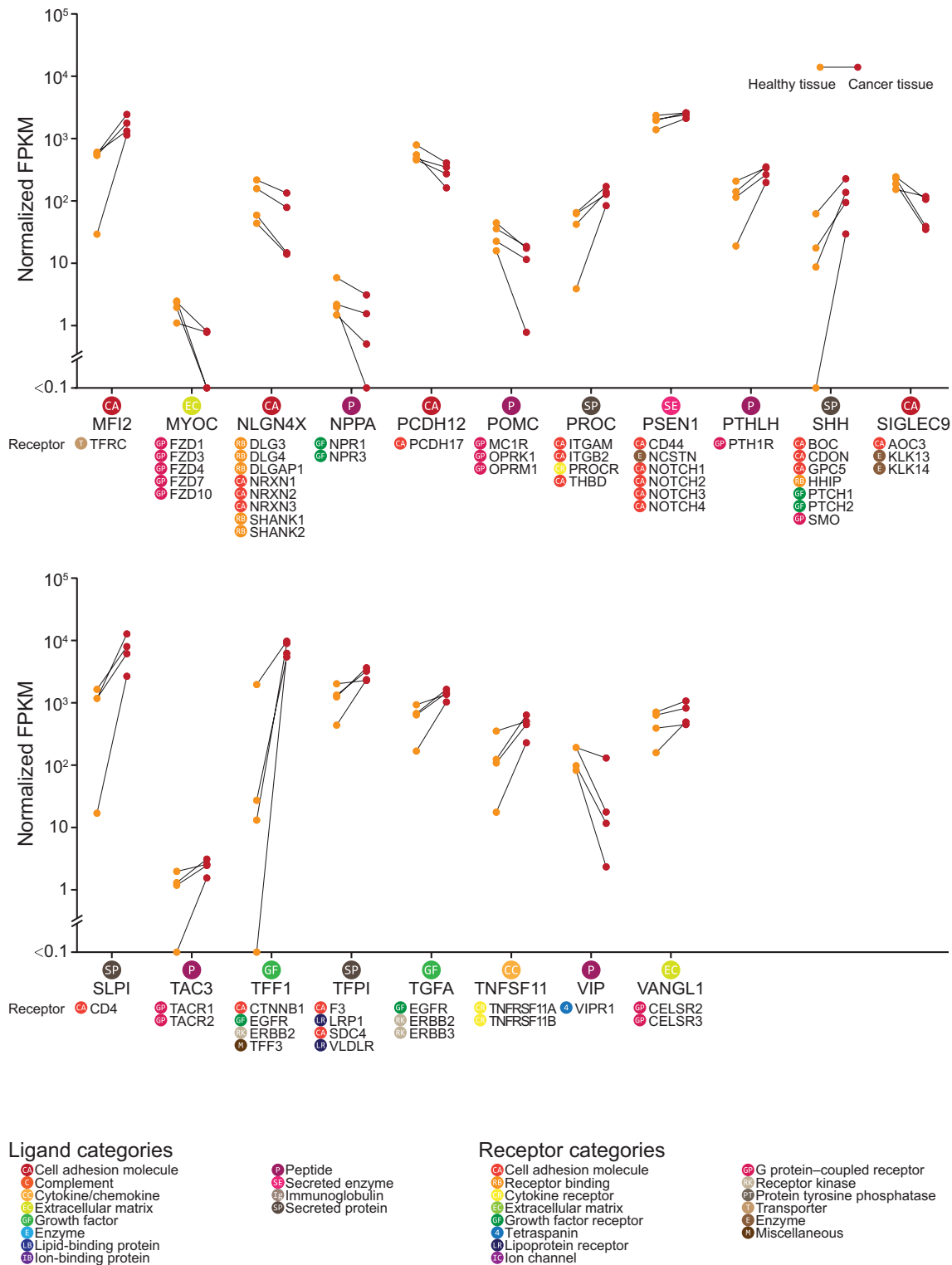


Fig. 8. DRG receptor-associated ligand expression in normal and malignant pancreatic tissue from humans, part II. Additional data from the interactome analysis on normal and malignant pancreatic tissue with hDRG, performed and analyzed as described in Fig. 7, continued here in alphabetical order.

level, including in disease states, will ultimately be needed to achieve this goal. Such efforts are well under way and the technology to do such studies at the individual patient level are rapidly becoming available (82).

Another key finding is the degree to which ECM and cell adhesion molecules govern ligand-receptor interactions between peripheral cells and sensory neurons. These interactions dominated our

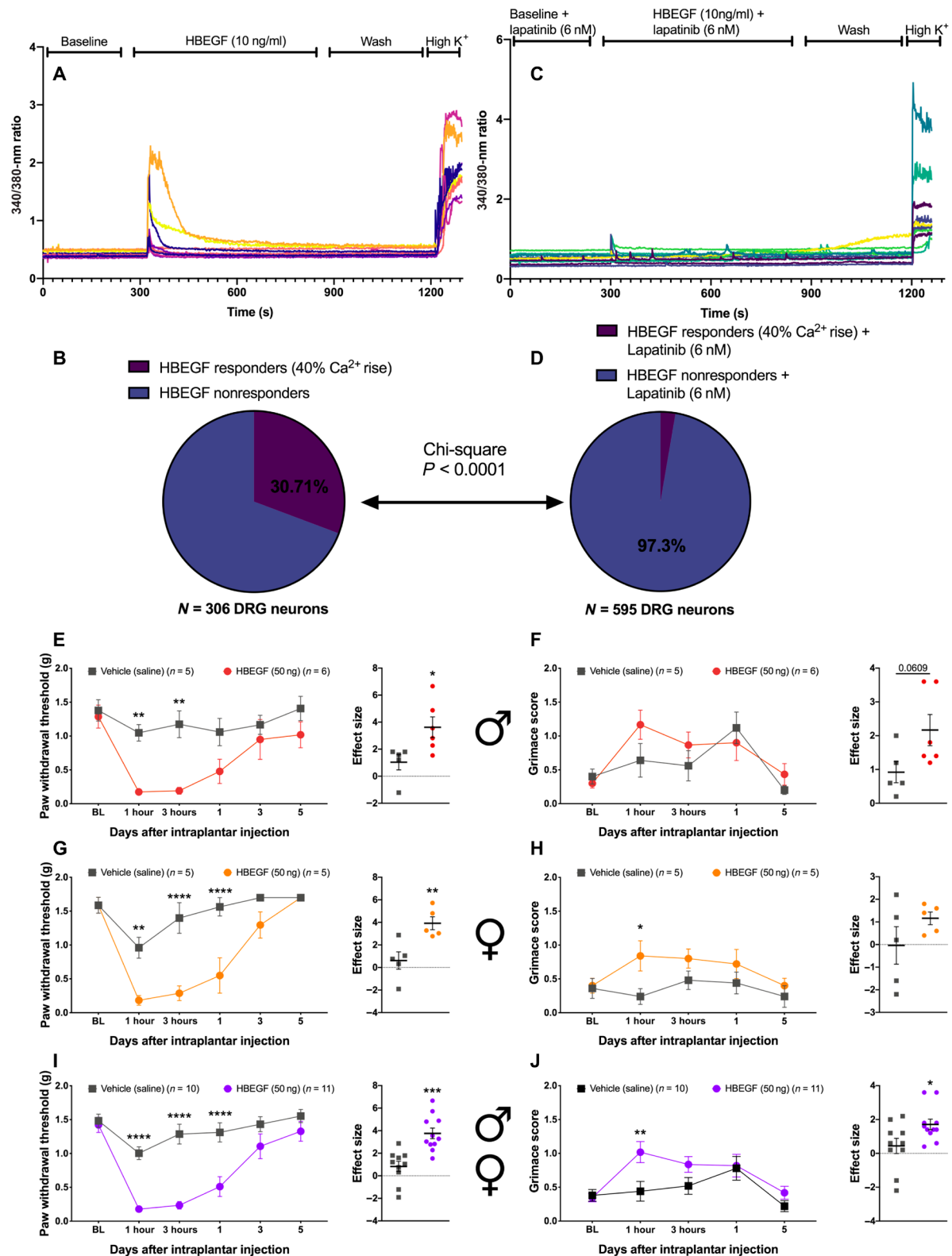


Fig. 9. HBEGF excites mDRG neurons and causes pain in vivo. (A to D) Intracellular Ca²⁺ concentration in mouse male and female DRG neurons in response to HBEGF [(A), analyzed in (B)] or HBEGF with the EGFR antagonist lapatinib [(C), analyzed in (D)]. N = 306 and 595 neurons, respectively. (E to J) Mechanical sensitivity to von Frey filaments, as inferred from paw withdrawal thresholds and grimacing, in male ICR mice (E and F) and female C57BL/6 mice (G and H) 1 hour after hind paw injection with saline or 50 ng of HBEGF. Pooled data for all male and female are displayed in (I) and (J). n = 5 to 11 mice each, as noted in the figure. *P < 0.05, **P < 0.01, and ****P < 0.001 by two-way ANOVA with Bonferroni posttest, or t test for effect size. Sample sizes are shown in the figure. Horizontal bars or boxes represent the mean, and error bars represent SEM. BL, baseline.

ligand-receptor interactomes, and many of these interactions have not been studied at all in the context of sensory neurobiology. Several studies in the past decade have pointed out the key role that ECM molecules play in the development of chronic pain states (51, 87, 88), but, again, these studies have only focused on a small number of the many interactions that were apparent in our interactomes. These ECM and adhesion molecule interactions may also play a critical role in recruitment and proliferation of immune cells to peripheral nerves and the DRG after nerve injury. Insofar as these neuroimmune interactions in the periphery are emerging as key players in nerve regeneration (41) and neuropathic pain (40, 89), gaining a better understanding of how this occurs will yield new insight into disease states. Therefore, this is almost certainly an area that is ripe for further exploration from the perspective of fundamental neurobiology knowledge and therapeutic target discovery.

A theme emerging from our interactomes built using sequencing data from human disease was the involvement of ErbB family receptors and their corresponding ligands. Previous studies have implicated the pathway associated with this family of receptors with chronic pain, but to our knowledge, HBEGF has not been specifically studied in this context. Genetic associations studies link the ErbB family of receptors and the ligand EREG (encoded by the *EREG* gene) to chronic temporomandibular joint pain (23). Animal pain models suggest that ErbB family activation by EREG promotes inflammatory and neuropathic pain and that ErbB receptor family signaling is critical for pain-promoting effects of opioids (23, 72). Last, several clinical trials have been done with inhibitors that target ErbB family receptors for neuropathic pain, and some of these have been positive (21, 22, 24). Our results point to a diversity of ligands specific to the ErbB family of receptors that are increased in abundance in painful tissues such as joints of people with RA and in pancreatic cancer. These ligands were distinct in these clinical cohorts and did not include EREG, whose ortholog is reported to be unique among ErbB receptor ligands in sensitizing nociceptors in mice (23). Some of them did include HBEGF, and we show here using mice that HBEGF can activate mDRG neurons in an ErbB receptor family-dependent fashion to cause pain in vivo. In mice, DRG neurons do not apparently express *Egfr*, but both PEP and NP nociceptors express *ErbB2* (12). HBEGF induced Ca^{2+} transients in mDRG neurons that were completely blocked by lapatinib, which inhibits both EGFR and ErbB2. It is very likely that pain-promoting effects of HBEGF in mice are mediated by ErbB2. In hDRG, however, both *EGFR* and *ERBB2* genes are expressed (14, 90), suggesting a potential species difference. Another consideration is that different ErbB family ligands have differential signaling bias when activating ErbB receptors in neurons, as shown by Martin and colleagues (23). It is likely necessary to study the effects of ErbB family ligands on human nociceptors because several published reports have demonstrated important differences between rodent and human nociceptors (19, 91–93). Nevertheless, our findings are promising from the perspective of broadening study of ErbB family receptor inhibitors for different chronic pain conditions. Our work highlights HBEGF, in addition to EREG, as EGFR agonists that may be involved in pathological pain.

There are some key limitations to our work. The first is that most of the interactomes presented are not precisely matched for the innervation of the target tissue. The exception is the colonic sensory neuron to enteric glia interactome. Future work will focus on building additional interactomes where the target cell types are matched to the subsets of nociceptors that specifically innervate those cells

and, if possible, taken from samples with the same pathophysiological state. This will have important implications for more precise target identification. The second is that single-cell resolution is not yet available for the hDRG, so the human disease-based interactomes should be interpreted with some caution. Our bulk-sequencing data affords a broad view of possible interactions between target tissues and hDRG neurons, but single-cell sequencing on hDRG neurons would improve confidence in targets emerging from these types of experiments. A third limitation is in gaps in the ligand-receptor interactome. Although we have made a concerted effort to include as many enzyme-derived small-molecule interactions as we can in this database, it is not comprehensive. There are also many ligand-receptor interactions that are not yet known, and these are necessarily not part of our interactome. Therefore, although our work elucidates many aspects of ligand-receptor interactions that are potentially involved in driving painful disease states, it cannot be viewed as a comprehensive resource. Last, although gene expression of ligands and receptors may predict signaling, posttranscriptional and posttranslational regulation—as well as mRNA and protein transport or localization—can modulate the degree and viability of such protein interactions. For candidate signaling pathways, interventional studies need to be performed to validate the predicted interactome. Our mouse HBEGF study provides a roadmap in how such studies may be designed. Nonetheless, our findings create a resource that may be built upon with further validation work and rapid advances in sequencing and other technologies. From this, we envision that new therapeutic targets specific to various chronic pain disorders may be identified.

MATERIALS AND METHODS

Mouse RNA-seq resources

The Tabula Muris dataset (10) contains scRNA-seq data generated by two methods: Smart-seq2 sequencing of specific cells using a fluorescence-activated cell sorting (FACS) method and a microfluidic emulsion method. The scRNA-seq data generated by the FACS method includes more tissue types and greater sensitivity (higher number of genes detected per cell); therefore, we used that data for our analysis. From all cell types identified in the Tabula Muris dataset, we selected cells from tissues that are strongly innervated by DRG neurons and identified 42 component cell types likely to interact directly with DRG-derived nerve endings and used these in our analysis. Details of the tissues and cell types found in the Tabula Muris dataset and which ones we chose for analysis in this work are located in data file S7.

scRNA-seq data from the mDRG (12) were used to generate the transcriptome profile of individual cell types within DRG. Expression values and metadata for each subpopulation of component cells provided in databases (L5_All.agg.loom) created by the original publication were used in our analysis. NFs (NF1 to NF3), NP neurons (NP1 to NP6), PEP neurons (PEP1 to PEP8), satellite glial cells (SATG1 to SATG2), and Schwann cells (SCHW) cell types from DRG tissue were selected for analysis. These were further grouped as described in Results.

Previously published RiboTag RNA-seq data of enteric glial cells from colon tissue were used (18). In this study, colonic inflammation was used to study how the active translome of enteric glia changes with inflammation. The RiboTag procedure driven by *Sox10-cre* was used to generate enteric glia translomes in vehicle-treated and colonic inflammation conditions. In turn, this was used to generate the interactome between colonic sensory neurons (details below)

and enteric glia. Raw sequencing data were provided by the authors of the original paper, mapped to gencode vM16 mouse genome annotation (94), and quantified using STAR 2.6.1c (95, 96). Read counts per gene per sample were provided as output by STAR and suitably normalized and used in downstream analysis.

Previously published scRNA-seq data of mDRG neurons retrogradely traced from colon (17) were used in the interactome analysis for colonic inflammation. Read counts per gene per cell, as well as cell-type labels (based on clustering) and gene marker information for cell types, were provided by the authors.

Human RNA-seq resources

hDRG tissue samples, previously sequenced using bulk RNA-seq and analyzed by our laboratory (14, 19), were used for quantifying the transcriptome profile of hDRG. Normalized read counts per gene [as transcripts per million (TPMs)] reported in those papers were used in the analysis here.

We analyzed data from Kuo *et al.* (16), who obtained scRNA-seq data from 940 human synovial CD14⁺ cells, enriched in macrophages, isolated from patients with RA and OA, to build the RA- and OA-associated interactomes. The original scRNA-seq data provided as read counts per gene per cell in the original publication and clustering-based cell-type labels for each cell were used. On the basis of the study by Kuo *et al.* (16), one cell cluster was enriched in RA samples when compared with OA samples (RA-enriched macrophages). Conversely, a second cluster was enriched in patients with OA when compared with patients with RA (OA-enriched macrophages). These two cell types were picked for the interactome analysis to compare macrophages from patients with RA versus macrophages from patients with OA.

Pancreatic cancer tissue bulk RNA-seq data were acquired from the TCGA database (20). Samples from individuals that had matched healthy and cancerous pancreatic tissue were used for analysis in this paper. There was a total of four pairs of samples in the TCGA pancreatic cancer database that fit the criteria, and all pairs were used. The TCGA database provides normalized read counts per gene [as fragments per kilobase per million mapped fragments (FPKM)], which was used for downstream analysis.

Reference annotation for receptor and ligand pairs

Ramilowski *et al.* (25) identified 2557 pairs of ligand-receptor interactions that were used as the basis for generating the full database of ligand-receptor pairs used here. To curate a more complete list of ligand- and receptor-like interactions, we manually curated and incremented this database as follows: Additional genes whose products are ligands and receptors were identified from gene annotation databases, like the Human Genome Organization (HUGO) (28) and AmiGO (30) databases, as well as the literature. Their corresponding signaling interaction partners were identified from the literature and an existing database (27).

It is to be noted that not all ligand-receptor pair interactions are directly encoded in the genome, so we added enzymes that are known to synthesize ligands to the ligand database and paired these with receptors for the synthesized ligand. Some interactions between proteins found at the surface of cells do not have a clear ligand-receptor relationship, for instance, in some ECM and cell adhesion protein interactions. In these cases, if one of the pair was expressed in the DRG (transcriptionally), the corresponding gene was included in the receptor database, and its interacting protein partner's gene name

was included in the ligand database. The COMPARTMENTS database (26) and literature was additionally used to filter out ligand-side proteins that are not known to be secreted or localized in the ECM.

Gene annotations for cell adhesion molecules, GPCR, growth factor, ion channels, neuropeptides, nuclear receptors, and receptor kinases obtained from the literature, the human HUGO (28), and human and mouse AMIGO (30) databases were used to additionally populate our database on top of the protein interaction lists by Ramilowski *et al.* (25). A total of 3098 pairs of ligand-receptor interactions are used in our interactome analysis (entire list shown in data file S8).

Gene relative abundance normalization

RNA-seq read counts per gene are typically normalized for gene length and whole-transcriptome coverage to quantify relative abundance of transcripts for each gene. We used several different normalization strategies on the basis of the public availability of read counts and normalized data, and what was the most appropriate normalization in the context of the analysis. Although there is some heterogeneity in normalization procedures across RNA-seq datasets that we analyzed, within each dataset, normalization was performed consistently using a single approach.

Gene abundances for the human pancreatic cancer samples in FPKM (obtained from the TCGA website) and RNA-seq data for hDRG samples in TPMs (obtained from the original paper) were used for downstream analysis. However, some of the RNA-seq datasets used in this paper were obtained as read counts per gene per sample (for bulk RNA-seq) or per cell (for scRNA-seq); thus, we normalized these using standard approaches (97). Because we did not explicitly compare expression levels across different genes, normalization by gene length was not performed as it does not influence our analysis. We calculated reads per million mapped reads (RPMs) for bulk RNA-seq and for scRNA-seq datasets that had lower transcriptome coverage, and upper-decile normalized RPM (udRPM) was used to normalize sequencing depth while accounting for coverage differences across multiple samples in low-sequencing depth situations (like scRNA-seq). RPM and udRPM of a gene were calculated with the following formulas

$$\text{RPM}_{\text{gene}} = \frac{R_{\text{gene}} \times 10^6}{\sum_{\text{gene}} R_{\text{gene}}}$$

where R_{gene} stands for the read counts for a specific gene and $\sum_{\text{gene}} R_{\text{gene}}$ stands for the read count sum of all genes.

$$\text{udRPM}_{\text{gene}} = \frac{\text{RPM}_{\text{gene}}}{90\text{th percentile of RPM}_{\text{gene}} \text{ within the sample}}$$

Interactome identification

Interactomes were predicted for ordered pairs of relevant tissues or cell types. On the basis of the biological context, we identified ligand-to-receptor signaling from one tissue or cell type to the other (unidirectional) or from each tissue or cell type to the other (bidirectional). The first step in building the interactome was to overlay ligand-encoding gene expression levels in all samples, cells in the tissue, or cell type wherein we investigate the upstream component of the signaling, and to similarly overlay the receptor-encoding gene expression levels in the tissue or cell type wherein we investigate the downstream component. Depending on the data available and the question being asked in each of our case studies, the

interactions were then ranked on the basis of ligand-side or receptor-side criteria (like degree of differential expression and specificity of expression in that tissue or cell type) and filtered out if the gene expression was not consistently detectable across biological replicates. Our approach uses gene expression levels as a surrogate for protein abundance levels, because of the difficulty of generating high-throughput and high signal-to-noise ratio protein abundance data.

Identification of cell type–restricted gene expression patterns in mouse scRNA-seq datasets

The Tabula Muris dataset was specifically analyzed to identify gene coexpression modules that were not expressed ubiquitously across all 42 relevant cell types in the database but restricted to a subset of them. To identify gene modules that were enriched in different cell types, a cell and gene biclustering was performed on the uDRPM per gene per cell-type matrix generated in the for the 42 cell types. The `scratch.heatmap` package from the Allen Institute (37) was used to generate clusters to identify gene modules.

The uDRPM matrix was first multiplied by 1000 (to limit the effect of adding a smoothing factor), and 1 was added to each element of the matrix before it was \log_2 -transformed. Such a log-transformed matrix is an approximation of the qualitative expression patterns of different genes across all 42 cell types.

We performed hierarchical clustering through a top-down approach, identifying a total of 8189 genes that were generically expressed across all preidentified cell types in the first round, which were labeled as ubiquitously expressed and set aside from the clustering. In the next round of clustering, another 5117 genes were identified to have low to no expression across all cell types and were excluded from the analysis. Distinct clusters of cell types and gene modules were identified in the final round of clustering, and genes from these coexpression modules that were restricted in expression to a subset of the cell types were used to characterize a “cell type–enriched” interactome. The parameters for each round of clustering are listed in data file S9.

Criteria for a gene to be considered detectable in a given cell type

Ligands and/or receptors were filtered in some of the interactomes for our case studies on the basis of whether reads were consistently detectable in biological replicates for one (or more) groups. Because scRNA-seq data usually have low sequencing depth per cell, trinarization scores were used to estimate whether a gene is expressed in a particular cell type. Briefly, the trinarization score, described previously by Zeisel *et al.* (12), is a formulation of the posterior probability whether a gene is detected in a cell type. The parameters used here in the calculation of the trinarization score were $f = 0.05$, $\alpha = 1.5$, and $\beta = 2$. Genes with probability $P > 0.95$ were considered expressed.

Criteria for identifying differential expression of gene relative abundance

In addition, ligand and receptor genes are ranked by degree of differential expression in interactomes of some of our case studies. Although traditional statistical hypothesis testing is the norm for identifying differential expression, in experimental setups involving limited replication, differential expression analysis can be performed using related statistics like the strictly standardized mean difference (SSMD) or Bhattacharyya distance, which take both between and within group variance into account when ranking genes by differential expression.

The SSMD (98, 99) was used to characterize the difference in means of two groups, controlled by within-group variability, and was used to estimate effect size between two different groups under comparison, using the following formula

$$\text{SSMD} = \frac{\mu_p - \mu_q}{\sqrt{\sigma_q^2 + \sigma_p^2}}$$

where in a particular gene, for two groups p and q , σ^2 stands for the variance, and μ stands for mean of the gene expression levels across libraries for each group in question (represented by a subscript).

The Bhattacharyya distance (90, 100) was used to calculate the similarity of the probability distributions of scRNA-seq data from two different conditions using the following formula. The related Bhattacharyya coefficient (derived from the Bhattacharyya distance D_B) was used to calculate the amount of overlap in the area under the curve of the two sample distributions being compared

$$D_B(p, q) = \frac{1}{4} \ln \left(\frac{1}{4} \left(\frac{\sigma_p^2}{\sigma_q^2} + \frac{\sigma_q^2}{\sigma_p^2} + 2 \right) \right) + \frac{1}{4} \left(\frac{(\mu_p - \mu_q)^2}{\sigma_q^2 + \sigma_p^2} \right)$$

In this formula, D stands for distance, p and q stand for gene expression level across all cells in the first condition and second condition respectively, σ stands for SD, and μ stands for mean. Genes with a distance > 0.3 between two conditions of scRNA-seq were considered differentially expressed.

Interactome analysis methodological details for case studies

For analysis of the publicly available mouse scRNA-seq datasets, interactome analysis was performed between 42 cell types in tissues innervated by the DRG identified in the Tabula Muris dataset (10) and three broad classes of mDRG sensory neurons (top-level subpopulations of PEP, NP, and NF neurons, obtained by merging all subcategories under them on the basis of hierarchical clustering) from the mDRG scRNA-seq study by Zeisel *et al.* (12). For each of the 42 Tabula Muris cell types and the three mDRG subpopulations from mousebrain.org, individual cells in these subcategories were pooled, and summed per-gene read counts were normalized to uDRPM to obtain a single value for each gene’s relative expression in each cell type.

In addition, on the basis of the biclustering of genes and cell types of the Tabula Muris dataset, 25 coexpression modules were identified that showed restricted expression across 18 classes of cell types over the 42 constituent cell types in Tabula Muris. Interactome analysis was then performed for each of the 42 Tabula Muris cell types to each of the three mouse sensory neuronal cell types. Last, interactomes were built using the set of genes present in the 25 gene coexpression modules having cell type–restricted expression in Tabula Muris to the three sensory neuronal subpopulations.

Interactomes were then filtered by the receptor gene expression level in DRG sensory neurons. Ligand–receptor interactions with receptor expression level < 0.001 uDRPM across all three types of sensory neurons (PEP, NF, and NP) were excluded from the results.

GO term analysis was performed on the ligand and receptor genes for the individual interactomes using Enrichr (31, 32), and the top five (ranked by adjusted P value) GO terms for GO biological process and GO molecular function were collected and shown. Data sheets are presented in data file S1, and results are visualized in Fig. 1.

Bidirectional interactome between different cell types within the mDRG

scRNA-seq mouse neuronal and glial subpopulations in the DRG scRNA-seq data (12) were further pooled into five main groups on the basis of how similar their expression profiles were: NF, NP, and PEP sensory neurons; satellite glial cells (SATG); and Schwann cells (SCHW). The mean of the normalized expression values across the related subpopulations was used for the expression level of each merged group, and uDRPMs were calculated. These were then used as the transcriptome profile of different cell types from the mDRG.

Interactome analysis on mDRG cell clusters was performed in two separate directions: ligands from neuronal cells (NF, NP, and PEP) signaling to receptors on glial cells (SCHW and SATG), and vice versa. All identified ligand-receptor interactions were filtered by whether the ligands and receptors were both expressed at the mRNA level in at least one source cell type. The trinarization score was calculated to determine whether a gene was to be considered expressed in a certain cell type (score > 0.95). Circle plots were generated to present these interactions using the Circos program (Figs. 3 and 4) (101), wherein each identified ligand and receptor interaction is represented on the plot. To better present how certain groups of ligands or receptors may interact with each other, the ligand-encoding and receptor-encoding genes on the circle plots were ordered by hierarchical biclustering (Euclidean distance, average distance between elements of two clusters used as representative distance between those clusters) of the ligand- and receptor-encoding genes based on their interactions with each other. In addition, each gene was identified as expressed in NF, NP, PEP, SATG, or SCHW and marked as such on the plot.

Interactome between retrogradely traced colonic sensory neurons and enteric glial cells in a colitis model

For the transcriptome of retrogradely traced colonic sensory neurons (17), reads from all cells of the same cell type were pooled together to generate the gene expression level per cell type (as RPM). The interactome was then generated between these seven cell types and enteric glial cells after vehicle or DNBS treatment (18). Ligand-receptor interactions were filtered by the following criteria: Ligand genes were required to be consistently expressed (>0.01 RPM) in enteric glial cells across all replicates in at least one condition (vehicle- or DNBS-treated); ligand-encoding genes were considered to be altered by treatment when the $|\text{SSMD}| > \mu_{\text{SSMD}} + 1.2\sigma_{\text{SSMD}}$; and last, receptor-encoding genes with trinarization score > 0.95. Putative interactions where the receptor genes were enriched in specific populations of colonic afferents are shown in Fig. 5. All ligand-receptor interactions are provided in data file S4.

Interactome between macrophages enriched in human RA synovial tissue versus OA, and hDRG

The interactome was generated between RA- or OA-enriched macrophages (16) and hDRG (14). Predicted ligand-receptor interactions were filtered by the following criteria: (i) Ligand-encoding genes were required to be considered expressed in either RA-enriched macrophages or OA-enriched macrophages using the trinarization score > 0.95; (ii) ligand-encoding genes were considered substantially differentially expressed between RA-enriched macrophages and OA-enriched macrophages, using Bhattacharyya distance > 0.3; and (iii) receptor genes were required to be consistently expressed (>0.1 TPM) in all three hDRG samples. Interactions where the ligand

genes were highly expressed in RA-enriched macrophages are presented in Fig. 6; the interactions with ligand-encoding genes highly expressed in OA-enriched macrophages are provided in sheets 1 and 2 of data file S5.

Interactome between human pancreatic cancer tissue and hDRG

The interactome was generated between four paired healthy and cancer tissue samples from patients with pancreatic cancer (TCGA) and hDRG samples (14). Ligand-receptor interactions were filtered by the following criteria: (i) Ligand genes were considered significantly increased in pancreatic cancer samples versus healthy samples by statistical testing (paired Student's *t* test, $P < 0.05$). Because the low sample size (four pairs) does not allow us to stringently perform multiple testing *P* value correction, an additional criterion was imposed that direction of change in ligand gene abundance had to be consistent for all four pairs of samples. (ii) Receptor genes were required to be consistently expressed (>0.1 TPM) in all three hDRG samples. All interactions that met the filtering criteria are presented in Figs. 7 and 8.

Animals

All animal protocols were approved by the University of Texas at Dallas Institutional Animal Care and Use Committee and were consistent with the National Institutes of Health guide. Mice were kept on a 12-hour light-dark cycle with food and water provided ad libitum. Both C57BL/6 and ICR mice were bred at The University of Texas at Dallas.

Experimental reagents

Recombinant human HBEGF (259-HE) was purchased from R&D Systems and reconstituted to 50 $\mu\text{g}/\text{ml}$ in 0.1% bovine serum albumin. For hind paw injections, stock HBEGF was diluted in 0.9% saline to 5 $\text{ng}/\mu\text{l}$. Hind paw injections (10 μl) were done with a 30-gauge needle (305106, BD Biosciences) and glass gastight syringe (80901, Hamilton Co.).

Behavioral methods

Male ICR mice and female C57BL/6 mice (7 to 9 weeks old) were used for behavioral experiments, and experimenters were blinded to treatment. Mice were habituated to acrylic (behavior boxes 11.4 cm by 7.6 cm by 7.6 cm) with a wire mesh bottom (1 cm^2) before experiments. Hind paw mechanical withdrawal thresholds were determined using calibrated von Frey filaments (Stoelting Co.) and the up-down method (102). As a measure of spontaneous pain, mouse grimace scale (MGS) scores were determined by observation of facial action units as described by Langford *et al.* (103). Facial action unit intensity ratings were averaged to yield a MGS score for each mouse at each time point.

DRG cultures

The neuronal cultures used in the calcium imaging, DRGs were dissected from adult male and female C57BL/6 mice and suspended in Hanks' balanced salt solution without calcium or magnesium before culturing. The DRGs were then enzymatically digested using collagenase A and collagenase D (each 1 mg/ml , from Roche) with papain (30 U/ml) for 20 min at 37°C. Following this, ganglion was suspended and triturated in 1 ml of Hanks' balanced salt solution. The solution was passed through a 70- μm cell strainer for the

removal of debris. The cells were then resuspended in Dulbecco's modified Eagle's medium/F12/GlutaMAX (Gibco) culture media nourished with 10% fetal bovine serum (SH30088.03, Hyclone) and 1% penicillin/streptomycin (15070-063, Gibco). Cells were plated on precoated poly-D-lysine dishes (P35GC-1.5-10-C, MatTek), which were additionally coated with laminin (L2020, Sigma-Aldrich). The plated cells were then kept undisturbed in an incubator for 2 hours to allow them to adhere. The cells were then supplemented with the same culture media as described above but with the addition of NGF (10 ng/ml; 01-125, Millipore) and 5-fluoro-2'-deoxyuridine (3 µg/ml) + uridine (7 µg/ml) (FRD + U; Sigma-Aldrich). Last, the cells were kept in an incubator with 5% CO₂ and maintained at 37°C for 48 hours before use.

Ca²⁺ imaging

The cultures prepared and plated as described previously remained undisturbed in the incubator for 48 hours after plating. Cells were then loaded with Fura-2 AM (1 µg/µl; 108964-32-5, Life Technologies) for 1 hour. In the case of the experiments performed with the lapatinib (6 nM; 6811, Tocris), the cells were incubated in the drug 30 min before loading with Fura-2 AM. After the incubation period, the Fura-2 AM solution was replaced with normal bath solution (135 mM NaCl, 5 mM KCl, 10 mM HEPES, 1 M CaCl₂, 1 M MgCl₂, and 2 M glucose, adjusted to pH 7.4 with *N*-methyl-glucamine, the osmolarity of 300 ± 5 mOsm). After a 30-min incubation in the bath, the cells were then treated with solution of HBEGF (10 ng/ml) for 10 min (104). The recordings were done using an Olympus IX73 inverted microscope at ×40 magnification and the MetaFluor Fluorescence Ratio Imaging Software. The cells that exhibited a 20% ratiometric change (340 nm/380 nm) in Ca²⁺ levels when subjected to KCl treatment were classified as neurons. From there, the neurons that exhibited a 40% ratiometric change in response to HBEGF treatment were considered as responsive.

Statistical analysis

Computational analysis was performed using MATLAB and MS Excel, and plots were made using MATLAB and GraphPad Prism. Identification of differentially expressed genes were performed using SSMDs and the Bhattacharyya distance. Presence or absence of gene expression in specific cell populations was estimated using the trinarization score, by estimating the posterior distribution using a β prior on Bernoulli trials (outcome determined by whether or not a gene is detected in individual cells of the population). Details of RNA-seq quantification and testing are present in the associated methods section. Differences in time series for Ca²⁺ concentration were tested using the chi-square test. For testing behavioral responses at different times, two-way analysis of variance (ANOVA) (for different times and treatment regimes) was performed, with Bonferroni posttest correction. Differences in effect size were tested using *t* tests.

SUPPLEMENTARY MATERIALS

stke.sciencemag.org/cgi/content/full/14/674/eabe1648/DC1

Fig. S1. A full interactome for ligand-receptor-mediated interactions from neurons to glial cells within the mDRG.

Fig. S2. A full interactome for ligand-receptor-mediated interactions from glial cells to neurons within the mDRG.

Data file S1. Ligand-receptor interactions in mDRG sensory neurons and each of the 42 cell types in mDRG-innervated tissues from Tabula Muris, along with GO annotations.

Data file S2. Ligand-receptor interactions in mDRG sensory neurons and subsets of 42 cell types in mDRG-innervated tissues from Tabula Muris, for ligands with cell type-restricted expression.

Data file S3. DRG-localized ligand-receptor interaction pairs between mDRG neurons and glial cells.

Data file S4. Ligand-receptor interactions in differentially expressed ligand genes in DNBS-treated enteric glia, and paired receptors in thoracolumbar or lumbosacral mDRG neurons.

Data file S5. Ligand-receptor interaction pairs in OA and RA macrophages and hDRG-expressed receptors.

Data file S6. Ligand-receptor interaction pairs in ligand genes differentially expressed in pancreatic tumors, and hDRG-expressed receptors.

Data file S7. Cell types and number of cells from Tabula Muris used for downstream analysis.

Data file S8. Complete ligand-receptor interaction database underlying the interactome prediction framework.

Data file S9. Parameters for hierarchical clustering of gene expression patterns in Tabula Muris cell types using *scratch.hicat*.

[View/request a protocol for this paper from Bio-protocol.](#)

REFERENCES AND NOTES

1. A. I. Basbaum, D. M. Bautista, G. Scherrer, D. Julius, Cellular and molecular mechanisms of pain. *Cell* **139**, 267–284 (2009).
2. C. J. Woolf, Q. Ma, Nociceptors—noxious stimulus detectors. *Neuron* **55**, 353–364 (2007).
3. A. E. Dubin, A. Patapoutian, Nociceptors: The sensors of the pain pathway. *J. Clin. Invest.* **120**, 3760–3772 (2010).
4. D. L. Bennett, C. G. Woods, Painful and painless channelopathies. *Lancet Neurol.* **13**, 587–599 (2014).
5. E. T. Walters, Adaptive mechanisms driving maladaptive pain: How chronic ongoing activity in primary nociceptors can enhance evolutionary fitness after severe injury. *Philos. Trans. R. Soc. Lond. B Biol. Sci.* **374**, 20190277 (2019).
6. D. B. Reichling, J. D. Levine, Critical role of nociceptor plasticity in chronic pain. *Trends Neurosci.* **32**, 611–618 (2009).
7. F. Denk, S. B. McMahon, I. Tracey, Pain vulnerability: A neurobiological perspective. *Nat. Neurosci.* **17**, 192–200 (2014).
8. T. J. Price, K. E. Inyang, Commonalities between pain and memory mechanisms and their meaning for understanding chronic pain. *Prog. Mol. Biol. Transl. Sci.* **131**, 409–434 (2015).
9. T. J. Price, M. S. Gold, From mechanism to cure: Renewing the goal to eliminate the disease of pain. *Pain Med.* **19**, 1525–1549 (2018).
10. The Tabula Muris Consortium; Overall coordination; Logistical coordination; Organ collection and processing; Library preparation and sequencing; Computational data analysis; Cell type annotation; Writing group; Supplemental text writing group; Principal investigators, Single-cell transcriptomics of 20 mouse organs creates a *Tabula Muris*. *Nature* **562**, 367–372 (2018).
11. D. Usoskin, A. Furlan, S. Islam, H. Abdo, P. Lonnerberg, D. Lou, J. Hjerling-Leffler, J. Haeggstrom, O. Kharchenko, P. V. Kharchenko, S. Linnarsson, P. Ernfors, Unbiased classification of sensory neuron types by large-scale single-cell RNA sequencing. *Nat. Neurosci.* **18**, 145–153 (2015).
12. A. Zeisel, H. Hochgerner, P. Lonnerberg, A. Johnson, F. Memic, J. van der Zwan, M. Haring, E. Braun, L. E. Borm, G. La Manno, S. Codeluppi, A. Furlan, K. Lee, N. Skene, K. D. Harris, J. Hjerling-Leffler, E. Arenas, P. Ernfors, U. Marklund, S. Linnarsson, Molecular architecture of the mouse nervous system. *Cell* **174**, 999–1014.e22 (2018).
13. M. Melé, P. G. Ferreira, F. Reverter, D. S. DeLuca, J. Monlong, M. Sammeth, T. R. Young, J. M. Goldmann, D. D. Pervouchine, T. J. Sullivan, R. Johnson, A. V. Segre, S. Djebali, A. Niarchou, GTEx Consortium, F. A. Wright, T. Lappalainen, M. Calvo, G. Getz, E. T. Dermitzakis, K. G. Ardlie, R. Guigó, Human genomics. The human transcriptome across tissues and individuals. *Science* **348**, 660–665 (2015).
14. P. Ray, A. Torck, L. Quigley, A. Wangzhou, M. Neiman, C. Rao, T. Lam, J. Y. Kim, T. H. Kim, M. Q. Zhang, G. Dussor, T. J. Price, Comparative transcriptome profiling of the human and mouse dorsal root ganglia: an RNA-seq-based resource for pain and sensory neuroscience research. *Pain* **159**, 1325–1345 (2018).
15. A. L. Roy, R. Conroy, J. Smith, Y. Yao, A. C. Beckel-Mitchener, J. M. Anderson, E. L. Wilder, Accelerating a paradigm shift: The common fund single cell analysis program. *Sci. Adv.* **4**, eaat8573 (2018).
16. D. Kuo, J. Ding, I. S. Cohn, F. Zhang, K. Wei, D. A. Rao, C. Roza, U. K. Sokhi, S. Shanaj, D. J. Oliver, A. P. Echeverria, E. F. DiCarlo, M. B. Brenner, V. P. Bykerk, S. M. Goodman, S. Raychaudhuri, G. Ratsch, L. B. Ivashkiv, L. T. Donlin, HBEGF(+) macrophages in rheumatoid arthritis induce fibroblast invasiveness. *Sci. Transl. Med.* **11**, eaau8587 (2019).
17. J. R. F. Hockley, T. S. Taylor, G. Callejo, A. L. Wilbrey, A. Gutteridge, K. Bach, W. J. Winchester, D. C. Bulmer, G. McMurray, E. S. J. Smith, Single-cell RNAseq reveals seven classes of colonic sensory neuron. *Gut* **68**, 633–644 (2019).
18. N. M. Delvalle, C. Dharshika, W. Morales-Soto, D. E. Fried, L. Gaudette, B. D. Gulbransen, Communication between enteric neurons, glia, and nociceptors underlies the effects of tachykinins on neuroinflammation. *Cell. Mol. Gastroenterol. Hepatol.* **6**, 321–344 (2018).

19. R. Y. North, Y. Li, P. Ray, L. D. Rhines, C. E. Tatsui, G. Rao, C. A. Johansson, H. Zhang, Y. H. Kim, B. Zhang, G. Dussor, T. H. Kim, T. J. Price, P. M. Dougherty, Electrophysiological and transcriptomic correlates of neuropathic pain in human dorsal root ganglion neurons. *Brain* **142**, 1215–1226 (2019).
20. K. Tomczak, P. Czerwinska, M. Wizerowicz, The Cancer Genome Atlas (TCGA): An immeasurable source of knowledge. *Contemp. Oncol.* **19**, A68–A77 (2015).
21. C. Kersten, M. G. Cameron, S. Mjalnd, Epithelial growth factor receptor (EGFR)-inhibition for relief of neuropathic pain-A case series. *Scand J Pain* **4**, 3–7 (2013).
22. C. Kersten, M. G. Cameron, B. Laird, S. Mjalnd, Epidermal growth factor receptor-inhibition (EGFR-I) in the treatment of neuropathic pain. *Br. J. Anaesth.* **115**, 761–767 (2015).
23. L. J. Martin, S. B. Smith, A. Khoutorsky, C. A. Magnussen, A. Samoshkin, R. E. Sorge, C. Cho, N. Yosefpour, S. Sivaselvachandran, S. Tohyama, T. Cole, T. M. Khuong, E. Mir, D. G. Gibson, J. S. Wieskopf, S. G. Sotocinal, J. S. Austin, C. B. Meloto, J. H. Gitt, C. Gkogkas, N. Sonenberg, J. D. Greenspan, R. B. Fillingim, R. Ohrbach, G. D. Slade, C. Knott, R. Dubner, A. G. Mackley, A. Ribeiro-da-Silva, G. G. Neely, W. Maixner, D. V. Zaykin, J. S. Mogil, L. Diatchenko, Epiregulin and EGFR interactions are involved in pain processing. *J. Clin. Invest.* **127**, 3353–3366 (2017).
24. C. Kersten, M. G. Cameron, A. G. Bailey, M. T. Fallon, B. J. Laird, V. Paterson, R. Mitchell, S. M. Fleetwood-Walker, F. Daly, S. Mjalnd, Relief of neuropathic pain through epidermal growth factor receptor inhibition: A randomized proof-of-concept trial. *Pain Med.* **20**, 2495–2505 (2019).
25. J. A. Ramilowski, T. Goldberg, J. Harshbarger, E. Kloppman, M. Lizio, V. P. Satagopam, M. Itoh, H. Kawaji, P. Carninci, B. Rost, A. R. R. Forrest, A draft network of ligand–receptor-mediated multicellular signalling in human. *Nat. Commun.* **6**, 7866 (2015).
26. J. X. Binder, S. Pletscher-Frankild, K. Tsafou, C. Stolte, S. I. O'Donoghue, R. Schneider, L. J. Jensen, COMPARTMENTS: Unification and visualization of protein subcellular localization evidence. *Database* **2014**, bau012 (2014).
27. D. Szklarczyk, A. L. Gable, D. Lyon, A. Junge, S. Wyder, J. Huerta-Cepas, M. Simonovic, N. T. Doncheva, J. H. Morris, P. Bork, L. J. Jensen, C. V. Mering, STRING v11: Protein–protein association networks with increased coverage, supporting functional discovery in genome-wide experimental datasets. *Nucleic Acids Res.* **47**, D607–D613 (2019).
28. B. Yates, B. Braschi, K. A. Gray, R. L. Seal, S. Tweedie, E. A. Bruford, Genenames.org: The HGNC and VGNC resources in 2017. *Nucleic Acids Res.* **45**, D619–D625 (2017).
29. B. Braschi, P. Denny, K. Gray, T. Jones, R. Seal, S. Tweedie, B. Yates, E. Bruford, Genenames.org: The HGNC and VGNC resources in 2019. *Nucleic Acids Res.* **47**, D786–D792 (2019).
30. S. Carbon, A. Ireland, C. J. Mungall, S. Shu, B. Marshall, S. Lewis; AmiGO Hub; Web Presence Working Group, AmiGO: Online access to ontology and annotation data. *Bioinformatics* **25**, 288–289 (2009).
31. E. Y. Chen, C. M. Tan, Y. Kou, Q. N. Duan, Z. C. Wang, G. V. Meirelles, N. R. Clark, A. Ma'ayan, Enrichr: Interactive and collaborative HTML5 gene list enrichment analysis tool. *Bmc Bioinformatics* **14**, 128 (2013).
32. M. V. Kuleshov, M. R. Jones, A. D. Rouillard, N. F. Fernandez, Q. N. Duan, Z. C. Wang, S. Koplev, S. L. Jenkins, K. M. Jagodnik, A. Lachmann, M. G. McDermott, C. D. Monteiro, G. W. Gundersen, A. Ma'ayan, Enrichr: A comprehensive gene set enrichment analysis web server 2016 update. *Nucleic Acids Res.* **44**, W90–W97 (2016).
33. R.-R. Ji, R. W. T. Gereau IV, M. Malcangio, G. R. Strichartz, MAP kinase and pain. *Brain Res. Rev.* **60**, 135–148 (2009).
34. J. K. Moy, A. Khoutorsky, M. N. Asiedu, B. J. Black, J. L. Kuhn, P. Barragan-Iglesias, S. Megat, M. D. Burton, C. C. Burgos-Vega, O. K. Melemedjian, S. Boitano, J. Wagner, C. G. Gkogkas, J. J. Pancrazio, J. S. Mogil, G. Dussor, N. Sonenberg, T. J. Price, The MNK-eIF4E signaling axis contributes to injury-induced nociceptive plasticity and the development of chronic pain. *J. Neurosci.* **37**, 7481–7499 (2017).
35. O. A. Dina, G. C. McCarter, C. de Coupade, J. D. Levine, Role of the sensory neuron cytoskeleton in second messenger signaling for inflammatory pain. *Neuron* **39**, 613–624 (2003).
36. Z. Y. Zhuang, H. Xu, D. E. Clapham, R. R. Ji, Phosphatidylinositol 3-kinase activates ERK in primary sensory neurons and mediates inflammatory heat hyperalgesia through TRPV1 sensitization. *J. Neurosci.* **24**, 8300–8309 (2004).
37. B. Tasic, Z. Yao, L. T. Graybeck, K. A. Smith, T. N. Nguyen, D. Bertagnolli, J. Goldy, E. Garren, M. N. Economo, S. Viswanathan, O. Penn, T. Bakken, V. Menon, J. Miller, O. Fong, K. E. Hirokawa, K. Lathia, C. Rimorin, M. Tieu, R. Larsen, T. Casper, E. Barkan, M. Kroll, S. Parry, N. V. Shapovalova, D. Hirschstein, J. Pendergraft, H. A. Sullivan, T. K. Kim, A. Szafer, N. Dee, P. Groblewski, I. Wickersham, A. Cetin, J. A. Harris, B. P. Levi, S. M. Sunkin, L. Madisen, T. L. Daigle, L. Looger, A. Bernard, J. Phillips, E. Lein, M. Hawrylycz, K. Svoboda, A. R. Jones, C. Koch, H. Zeng, Shared and distinct transcriptomic cell types across neocortical areas. *Nature* **563**, 72–78 (2018).
38. R. E. Sorge, J. C. Mapplebeck, S. Rosen, S. Beggs, S. Taves, J. K. Alexander, L. J. Martin, J.-S. Austin, S. G. Sotocinal, D. Chen, M. Yang, X. Q. Shi, H. Huang, N. J. Pillon, P. J. Bilan, Y. Tu, A. Klip, R.-R. Ji, J. Zhang, M. W. Salter, J. S. Mogil, Different immune cells mediate mechanical pain hypersensitivity in male and female mice. *Nat. Neurosci.* **18**, 1081–1083 (2015).
39. S. F. Rosen, B. Ham, M. Haichin, I. C. Walters, S. Tohyama, S. G. Sotocinal, J. S. Mogil, Increased pain sensitivity and decreased opioid analgesia in T-cell-deficient mice and implications for sex differences. *Pain* **160**, 358–366 (2019).
40. X. Yu, H. Liu, K. A. Hamel, M. G. Morvan, S. Yu, J. Leff, Z. Guan, J. M. Braz, A. I. Basbaum, Dorsal root ganglion macrophages contribute to both the initiation and persistence of neuropathic pain. *Nat. Commun.* **11**, 264 (2020).
41. A. J. Davies, H. W. Kim, R. Gonzalez-Cano, J. Choi, S. K. Back, S. E. Roh, E. Johnson, M. Gabriac, M. S. Kim, J. Lee, J. E. Lee, Y. S. Kim, Y. C. Bae, S. J. Kim, K. M. Lee, H. S. Na, P. Riva, A. Latremoliere, S. Rinaldi, S. Ugolini, M. Costigan, S. B. Oh, Natural killer cells degenerate intact sensory afferents following nerve injury. *Cell* **176**, 716–728.e18 (2019).
42. H. L. Willemen, N. Eijkelkamp, A. Garza Carbajal, H. Wang, M. Mack, J. Zijlstra, C. J. Heijnen, A. Kavelaars, Monocytes/macrophages control resolution of transient inflammatory pain. *J. Pain* **15**, 496–506 (2014).
43. K. Krukowski, N. Eijkelkamp, G. Laumet, C. E. Hack, Y. Li, P. M. Dougherty, C. J. Heijnen, A. Kavelaars, CD8+ T cells and endogenous IL-10 are required for resolution of chemotherapy-induced neuropathic pain. *J. Neurosci.* **36**, 11074–11083 (2016).
44. V. I. Shubayev, M. Angert, J. Dolkas, W. M. Campana, K. Palenscar, R. R. Myers, TNF α -induced MMP-9 promotes macrophage recruitment into injured peripheral nerve. *Mol. Cell. Neurosci.* **31**, 407–415 (2006).
45. S. M. Sweitzer, R. W. Colburn, M. Rutkowski, J. A. DeLeo, Acute peripheral inflammation induces moderate glial activation and spinal IL-1 β expression that correlates with pain behavior in the rat 1 published on the world wide web on 17 March 1999.1. *Brain Res.* **829**, 209–221 (1999).
46. A. Garza Carbajal, A. Ebersberger, A. Thiel, L. Ferrari, J. Acuna, S. Brosig, J. Isensee, K. Moeller, M. Siobal, S. Rose-John, J. Levine, H.-G. Schaible, T. Hucho, Oncostatin M induces hyperalgesic priming and amplifies signaling of cAMP to ERK by RapGEF2 and PKA. *J. Neurochem.* 10.1111/jnc.15172, (2020).
47. P. M. Grace, M. R. Hutchinson, S. F. Maier, L. R. Watkins, Pathological pain and the neuroimmune interface. *Nat. Rev. Immunol.* **14**, 217–231 (2014).
48. N. P. Gonçalves, C. B. Vægter, L. T. Pallesen, Peripheral glial cells in the development of diabetic neuropathy. *Front. Neurol.* **9**, 268 (2018).
49. J. B. P. Lemes, T. de Campos Lima, D. O. Santos, A. F. Neves, F. S. de Oliveira, C. A. Parada, C. M. da Cruz Lotufo, Participation of satellite glial cells of the dorsal root ganglia in acute nociception. *Neurosci. Lett.* **676**, 8–12 (2018).
50. S. E. Jager, L. T. Pallesen, M. Richner, P. Harley, Z. Hore, S. McMahon, F. Denk, C. B. Vægter, Changes in the transcriptional fingerprint of satellite glial cells following peripheral nerve injury. *Glia* **68**, 1375–1395 (2020).
51. M. Parisien, A. Samoshkin, S. N. Tansley, M. H. Piltonen, L. J. Martin, N. El-Hachem, C. Dagostino, M. Allegri, J. S. Mogil, A. Khoutorsky, L. Diatchenko, Genetic pathway analysis reveals a major role for extracellular matrix organization in inflammatory and neuropathic pain. *Pain* **160**, 932–944 (2019).
52. T. Hucho, J. D. Levine, Signaling pathways in sensitization: Toward a nociceptor cell biology. *Neuron* **55**, 365–376 (2007).
53. F. Madiai, V. M. Goettl, S.-R. Hussain, A. R. Clairmont, R. L. Stephens Jr., K. V. Hackshaw, Anti-fibroblast growth factor-2 antibodies attenuate mechanical allodynia in a rat model of neuropathic pain. *J. Mol. Neurosci.* **27**, 315–324 (2005).
54. H. Yamanaka, K. Obata, K. Kobayashi, Y. Dai, T. Fukuoka, K. Noguchi, Activation of fibroblast growth factor receptor by axotomy, through downstream p38 in dorsal root ganglion, contributes to neuropathic pain. *Neuroscience* **150**, 202–211 (2007).
55. M. Furusho, J. L. Dupree, M. Bryant, R. Bansal, Disruption of fibroblast growth factor receptor signaling in nonmyelinating Schwann cells causes sensory axonal neuropathy and impairment of thermal pain sensitivity. *J. Neurosci.* **29**, 1608–1614 (2009).
56. D. L. Hay, M. L. Garelja, D. R. Poyner, C. S. Walker, Update on the pharmacology of calcitonin/CGRP family of peptides: IUPHAR Review 25. *Br. J. Pharmacol.* **175**, 3–17 (2018).
57. O. Barkai, S. Puig, S. Lev, B. Title, B. Katz, L. Eli-Berchoer, H. B. Gutstein, A. M. Binshtok, Platelet-derived growth factor activates nociceptive neurons by inhibiting M-current and contributes to inflammatory pain. *Pain* **160**, 1281–1296 (2019).
58. R. Lopez-Bellido, S. Puig, P. J. Huang, C. R. Tsai, H. N. Turner, M. J. Galko, H. B. Gutstein, Growth factor signaling regulates mechanical nociception in flies and vertebrates. *J. Neurosci.* **39**, 6012–6030 (2019).
59. J. Zhao, A. Seereeram, M. A. Nassar, A. Levato, S. Pezet, G. Hathaway, C. Morenilla-Palao, C. Stirling, M. Fitzgerald, S. B. McMahon, M. Rios, J. N. Wood; London Pain Consortium, Nociceptor-derived brain-derived neurotrophic factor regulates acute and inflammatory but not neuropathic pain. *Mol. Cell. Neurosci.* **31**, 539–548 (2006).
60. S. Sikandar, M. S. Minett, Q. Millet, S. Santana-Varela, J. Lau, J. N. Wood, J. Zhao, Brain-derived neurotrophic factor derived from sensory neurons plays a critical role in chronic pain. *Brain* **141**, 1028–1039 (2018).

61. P. Wang, C. Du, F. X. Chen, C. Q. Li, Y. B. Yu, T. Han, S. Akhtar, X. L. Zuo, X. D. Tan, Y. Q. Li, BDNF contributes to IBS-like colonic hypersensitivity via activating the enteroglia-nerve unit. *Sci. Rep.* **6**, 20320 (2016).
62. Y. B. Yu, X. L. Zuo, Q. J. Zhao, F. X. Chen, J. Yang, Y. Y. Dong, P. Wang, Y. Q. Li, Brain-derived neurotrophic factor contributes to abdominal pain in irritable bowel syndrome. *Gut* **61**, 685–694 (2012).
63. Z. W. Zhu, H. Friess, L. Wang, A. Zimmermann, M. W. Buchler, Brain-derived neurotrophic factor (BDNF) is upregulated and associated with pain in chronic pancreatitis. *Dig. Dis. Sci.* **46**, 1633–1639 (2001).
64. K. M. Albers, C. J. Woodbury, A. M. Ritter, B. M. Davis, H. R. Koerber, Glial cell-line-derived neurotrophic factor expression in skin alters the mechanical sensitivity of cutaneous nociceptors. *J. Neurosci.* **26**, 2981–2990 (2006).
65. S. A. Malin, D. C. Molliver, H. R. Koerber, P. Cornuet, R. Frye, K. M. Albers, B. M. Davis, Glial cell line-derived neurotrophic factor family members sensitize nociceptors in vitro and produce thermal hyperalgesia in vivo. *J. Neurosci.* **26**, 8588–8599 (2006).
66. L. F. Queme, A. A. Weyler, E. R. Cohen, R. C. Hudgins, M. P. Jankowski, A dual role for peripheral GDNF signaling in nociception and cardiovascular reflexes in the mouse. *Proc. Natl. Acad. Sci. U.S.A.* **117**, 698–707 (2020).
67. J. J. DeBerry, J. L. Saloman, B. K. Dragoo, K. M. Albers, B. M. Davis, Artemin immunotherapy is effective in preventing and reversing cystitis-induced bladder hyperalgesia via TRPA1 regulation. *J. Pain* **16**, 628–636 (2015).
68. D. C. Bulmer, D. Grundy, Achieving translation in models of visceral pain. *Curr. Opin. Pharmacol.* **11**, 575–581 (2011).
69. M. P. Klinck, J. S. Mogil, M. Moreau, B. D. X. Lascelles, P. A. Flecknell, T. Poitte, E. Troncy, Translational pain assessment: Could natural animal models be the missing link? *Pain* **158**, 1633–1646 (2017).
70. S. Yamane, S. Ishida, Y. Hanamoto, K.-I. Kumagai, R. Masuda, K. Tanaka, N. Shiobara, N. Yamane, T. Mori, T. Juji, N. Fukui, T. Itoh, T. Ochi, R. Suzuki, Proinflammatory role of amphiregulin, an epidermal growth factor family member whose expression is augmented in rheumatoid arthritis patients. *J. Inflamm.* **5**, 5 (2008).
71. M. Harada, D. Kamimura, Y. Arima, H. Kohsaka, Y. Nakatsuji, M. Nishida, T. Atsumi, J. Meng, H. Bando, R. Singh, L. Sabharwal, J.-J. Jiang, N. Kumai, N. Miyasaka, S. Sakoda, K. Yamauchi-Takahara, H. Ogura, T. Hirano, M. Murakami, Temporal expression of growth factors triggered by epiregulin regulates inflammation development. *J. Immunol.* **194**, 1039–1046 (2015).
72. S. Puig, C. L. Donica, H. B. Gutstein, EGFR signaling causes morphine tolerance and mechanical sensitization in rats. *eNeuro* **7**, ENEURO.0460 (2020).
73. A. I. Catrina, C. I. Svensson, V. Malmstrom, G. Schett, L. Klareskog, Mechanisms leading from systemic autoimmunity to joint-specific disease in rheumatoid arthritis. *Nat. Rev. Rheumatol.* **13**, 79–86 (2017).
74. E. Krock, A. Jurczak, C. I. Svensson, Pain pathogenesis in rheumatoid arthritis-what have we learned from animal models? *Pain* **159** (Suppl 1), S98–S109 (2018).
75. C. D. Swanson, E. H. Akama-Garren, E. A. Stein, J. D. Petralia, P. J. Ruiz, A. Edalati, T. M. Lindstrom, W. H. Robinson, Inhibition of epidermal growth factor receptor tyrosine kinase ameliorates collagen-induced arthritis. *J. Immunol.* **188**, 3513–3521 (2012).
76. A. Caraceni, R. K. Portenoy, Pain management in patients with pancreatic carcinoma. *Cancer* **78**, 639–653 (1996).
77. A. M. Drewes, C. M. Campbell, G. O. Ceyhan, M. Delhay, P. K. Garg, H. van Goor, B. Laquente, B. Morlion, S. S. Olesen, V. K. Singh, P. Sjøgren, E. Szigethy, J. A. Windsor, M. G. Salvetti, R. Talukdar, Pain in pancreatic ductal adenocarcinoma: A multidisciplinary, International guideline for optimized management. *Pancreatol.* **18**, 446–457 (2018).
78. M. H. Kalsner, J. Barkin, J. M. Macintyre, Pancreatic cancer. Assessment of prognosis by clinical presentation. *Cancer* **56**, 397–402 (1985).
79. R. L. Krech, D. Walsh, Symptoms of pancreatic cancer. *J. Pain Symptom Manage.* **6**, 360–367 (1991).
80. A. Bezjak, D. Tu, L. Seymour, G. Clark, A. Trajkovic, M. Zukin, J. Ayoub, S. Lago, R. de Albuquerque Ribeiro, A. Gerogianni, A. Cyjon, J. Noble, F. Laberge, R. T. Chan, D. Fenton, J. von Pawel, M. Reck, F. A. Shepherd; National Cancer Institute of Canada Clinical Trials Group Study BR.21, Symptom improvement in lung cancer patients treated with erlotinib: quality of life analysis of the National Cancer Institute of Canada Clinical Trials Group Study BR.21. *J. Clin. Oncol.* **24**, 3831–3837 (2006).
81. J. W. Kim, H.-P. Kim, S.-A. Im, S. Kang, H. S. Hur, Y.-K. Yoon, D.-Y. Oh, J. H. Kim, D. S. Lee, T.-Y. Kim, Y.-J. Bang, The growth inhibitory effect of lapatinib, a dual inhibitor of EGFR and HER2 tyrosine kinase, in gastric cancer cell lines. *Cancer Lett.* **272**, 296–306 (2008).
82. R. Stark, M. Grzelak, J. Hadfield, RNA sequencing: The teenage years. *Nat. Rev. Genet.* **20**, 631–656 (2019).
83. E. Lein, L. E. Borm, S. Linnarsson, The promise of spatial transcriptomics for neuroscience in the era of molecular cell typing. *Science* **358**, 64–69 (2017).
84. J. Woodcock, J. Witter, R. A. Dionne, Stimulating the development of mechanism-based, individualized pain therapies. *Nat. Rev. Drug Discov.* **6**, 703–710 (2007).
85. M. T. Brown, F. T. Murphy, D. M. Radin, I. Davignon, M. D. Smith, C. R. West, Tanezumab reduces osteoarthritic knee pain: Results of a randomized, double-blind, placebo-controlled phase III trial. *J. Pain* **13**, 790–798 (2012).
86. H. Sun, D. W. Dodick, S. Silberstein, P. J. Goadsby, U. Reuter, M. Ashina, J. Saper, R. Cady, Y. Chon, J. Dietrich, R. Lenz, Safety and efficacy of AMG 334 for prevention of episodic migraine: A randomised, double-blind, placebo-controlled, phase 2 trial. *Lancet Neurol.* **15**, 382–390 (2016).
87. R. R. Ji, Z. Z. Xu, X. Wang, E. H. Lo, Matrix metalloproteinase regulation of neuropathic pain. *Trends Pharmacol. Sci.* **30**, 336–340 (2009).
88. D. B. Reichling, P. G. Green, J. D. Levine, The fundamental unit of pain is the cell. *Pain* **154** (Suppl 1), S2–S9 (2013).
89. R. R. Ji, A. Chamesian, Y. Q. Zhang, Pain regulation by non-neuronal cells and inflammation. *Science* **354**, 572–577 (2016).
90. A. Wangzhou, L. A. McIlvried, C. Paige, P. Barragan-Iglesias, S. Shiers, A. Ahmad, C. A. Guzman, G. Dussor, P. R. Ray, R. W. Gereau IV, T. J. Price, Pharmacological target-focused transcriptomic analysis of native vs cultured human and mouse dorsal root ganglia. *Pain* **161**, 1497–1517 (2020).
91. S. Davidsson, J. P. Golden, B. A. Copits, P. R. Ray, S. K. Vogt, M. V. Valtcheva, R. E. Schmidt, A. Ghetti, T. J. Price, R. W. Gereau IV, Group II mGluRs suppress hyperexcitability in mouse and human nociceptors. *Pain* **157**, 2081–2088 (2016).
92. C. Rostock, K. Schrenk-Siemens, J. Pohle, J. Siemens, Human vs. mouse nociceptors – Similarities and differences. *Neuroscience* **387**, 13–27 (2018).
93. J. K. Moy, J. E. Hartung, M. G. Duque, R. Friedman, V. Nagarajan, E. Loeza-Alcocer, H. R. Koerber, T. Christoph, W. Schroder, M. S. Gold, Distribution of functional opioid receptors in human dorsal root ganglion neurons. *Pain* **161**, 1636–1649 (2020).
94. A. Frankish, M. Diekhans, A. M. Ferreira, R. Johnson, I. Jungreis, J. Loveland, J. M. Mudge, C. Sisu, J. Wright, J. Armstrong, I. Barnes, A. Berry, A. Bignell, S. C. Sala, J. Chrast, F. Cunningham, T. Di Domenico, S. Donaldson, I. T. Fiddes, C. G. Giron, J. M. Gonzalez, T. Goghan, M. Hardy, T. Hourlier, T. Hunt, O. G. Izuogu, J. Lagarde, F. J. Martin, L. Martinez, S. Mohan, P. Muir, F. C. P. Navarro, A. Parker, B. K. Pei, F. Pozo, M. Ruffier, B. M. Schmitt, E. Stapleton, M. M. Suner, I. Sycheva, B. Uszczynska-Ratajczak, J. Xu, A. Yates, D. Zerbino, Y. Zhang, B. Aken, J. S. Choudhary, M. Gerstein, R. Guigo, T. J. Hubbard, M. Kellis, B. Paten, A. Reymond, M. L. Tress, P. Flicek, GENCODE reference annotation for the human and mouse genomes. *Nucleic Acids Res.* **47**, D766–D773 (2019).
95. A. Dobin, C. A. Davis, F. Schlesinger, J. Drenkow, C. Zaleski, S. Jha, P. Batut, M. Chaisson, T. R. Gingeras, STAR: ultrafast universal RNA-seq aligner. *Bioinformatics* **29**, 15–21 (2013).
96. A. Dobin, T. R. Gingeras, Optimizing RNA-Seq Mapping with STAR. *Methods Mol. Biol.* **1415**, 245–262 (2016).
97. L. Pachter, Models for transcript quantification from RNA-Seq. arXiv:1104.3889 [q-bio.GN] (19 April 2011).
98. X. D. Zhang, A. S. Espeseth, N. Chung, D. J. Holder, M. Ferrer, *American Statistical Association Proceedings* (2006), pp. 882–886.
99. P. Ray, J. Kahn, A. Wangzhou, D. Tavares-Ferreira, A. N. Akopian, G. Dussor, T. J. Price, Transcriptome analysis of the human tibial nerve identifies sexually dimorphic expression of genes involved in pain, inflammation and neuro-immunity. *Front. Mol. Neurosci.* **12**, 37 (2019).
100. A. Bhattacharyya, On a measure of divergence between two statistical populations defined by their probability distributions. *Bull. Calcutta Math. Soc.* **35**, 99–109 (1943).
101. M. Krzywinski, J. Schein, I. Birol, J. Connors, R. Gascoyne, D. Horsman, S. J. Jones, M. A. Marra, Circos: An information aesthetic for comparative genomics. *Genome Res.* **19**, 1639–1645 (2009).
102. S. R. Chaplan, F. W. Bach, J. W. Pogrel, J. M. Chung, T. L. Yaksh, Quantitative assessment of tactile allodynia in the rat paw. *J. Neurosci. Methods* **53**, 55–63 (1994).
103. D. J. Langford, A. L. Bailey, M. L. Chanda, S. E. Clarke, T. E. Drummond, S. Echols, S. Glick, J. Ingrao, T. Klassen-Ross, M. L. Lacroix-Fralish, L. Matsumiya, R. E. Sorge, S. G. Sotocinal, J. M. Tabaka, D. Wong, A. M. van den Maagdenberg, M. D. Ferrari, K. D. Craig, J. S. Mogil, Coding of facial expressions of pain in the laboratory mouse. *Nat. Methods* **7**, 447–449 (2010).
104. J. M. Sanders, M. E. Wampole, M. L. Thakur, E. Wickstrom, Molecular determinants of epidermal growth factor binding: A molecular dynamics study. *PLOS ONE* **8**, e54136 (2013).

Acknowledgments: We would like to thank J. Hockley and E. St. John Smith for help with the colonic single neuron sequencing data, B. Gulbransen and laboratory for help with the enteric glia TRAP data, and Z. Xuan for clarifying TCGA metadata formats. We thank all the authors of the papers from which we used their sequencing data for their exemplary transparency in sharing the details of their work with us. **Funding:** NIH grants NS113457 (C.P.), NS065926 (T.J.P.), and NS102161 (T.J.P.). **Author contributions:** Conceived the project: G.D., P.R.R., and T.J.P. Performed experiments: A.W., C.P., S.V.N., D.K.N., M.K., and P.R.R. Supervised experiments:

G.D., P.R.R., and T.J.P. Analyzed data: A.W., C.P., D.K.N., M.K., and P.R.R. Drew figures: A.W. and C.P. Wrote and edited the manuscript: A.W., C.P., G.D., P.R.R., and T.J.P. All authors approved the final version of the manuscript. **Competing interests:** A.W., C.P., G.D., P.R.R., and T.J.P. are founders of Doloromics. **Data and materials availability:** Meta-analysis for this project was performed on publicly available RNA-seq datasets, as cited; no new RNA-seq datasets were generated for this study. All other data needed to evaluate the conclusions in the paper are present in the paper or the Supplementary Materials. We have filed a patent on the interactome algorithm through The University of Texas at Dallas.

Submitted 4 August 2020
Accepted 17 February 2021
Published 16 March 2021
10.1126/scisignal.abe1648

Citation: A. Wangzhou, C. Paige, S. V. Neerukonda, D. K. Naik, M. Kume, E. T. David, G. Dussor, P. R. Ray, T. J. Price, A ligand-receptor interactome platform for discovery of pain mechanisms and therapeutic targets. *Sci. Signal.* **14**, eabe1648 (2021).

A ligand-receptor interactome platform for discovery of pain mechanisms and therapeutic targets

Andi Wangzhou, Candler Paige, Sanjay V. Neerukonda, Dhananjay K. Naik, Moeno Kume, Eric T. David, Gregory Dussor, Pradipta R. Ray and Theodore J. Price

Sci. Signal. **14** (674), eabe1648.
DOI: 10.1126/scisignal.abe1648

Painful connections

Chronic pain impairs quality of life, is challenging to treat, and accompanies various diseases. Wangzhou *et al.* integrated bulk and single-cell RNA sequencing of ligand and receptor gene expression in the dorsal root ganglion (DRG) and various peripheral cell types from humans and mice. Computational analysis of these data enabled the construction of a connectome of potential and cell type-specific interaction points between sensory nerves and innervated tissues. With validation in a mouse model of mechanical pain, their findings suggest that blocking heparin-binding epidermal growth factor (HBEGF) signaling may be a common and effective way to alleviate chronic pain in arthritis, colitis, and pancreatic cancer. The resource and the approach, in general, may be used to predict mechanisms of cell-cell communication between various tissues and cell types.

ARTICLE TOOLS	http://stke.sciencemag.org/content/14/674/eabe1648
SUPPLEMENTARY MATERIALS	http://stke.sciencemag.org/content/suppl/2021/03/12/14.674.eabe1648.DC1
RELATED CONTENT	http://stke.sciencemag.org/content/sigtrans/13/630/eaaz1854.full http://stke.sciencemag.org/content/sigtrans/13/638/eaaw1519.full http://science.sciencemag.org/content/sci/369/6505/774.full http://stm.sciencemag.org/content/scitransmed/11/491/eaau8587.full http://stm.sciencemag.org/content/scitransmed/13/576/eabb3946.full
REFERENCES	This article cites 101 articles, 19 of which you can access for free http://stke.sciencemag.org/content/14/674/eabe1648#BIBL
PERMISSIONS	http://www.sciencemag.org/help/reprints-and-permissions

Use of this article is subject to the [Terms of Service](#)

Science Signaling (ISSN 1937-9145) is published by the American Association for the Advancement of Science, 1200 New York Avenue NW, Washington, DC 20005. The title *Science Signaling* is a registered trademark of AAAS.

Copyright © 2021 The Authors, some rights reserved; exclusive licensee American Association for the Advancement of Science. No claim to original U.S. Government Works